PMEL Tsunami Forecast Series: Vol. 72

A Tsunami Forecast Model for Arecibo, Puerto Rico

Diego Arcas[1,2]

[1]Joint Institute for the Study of the Atmosphere and Ocean (JISAO), University of Washington, Seattle, WA

[2]NOAA/Pacific Marine Environmental Laboratory (PMEL), Seattle, WA

November 20, 2014

Contents

List of Figures

List of Tables

Foreword

Tsunamis have been recognized as a potential hazard to United States coastal communities since the mid-twentieth century, when multiple destructive tsunamis caused damage to the states of Hawaii, Alaska, California, Oregon, and Washington. In response to these events, the United States, under the auspices of the National Oceanic and Atmospheric Administration (NOAA), established the Pacific and Alaska Tsunami Warning Centers, dedicated to protecting United States interests from the threat posed by tsunamis. NOAA also created a tsunami research program at the Pacific Marine Environmental Laboratory (PMEL) to develop improved warning products.

The scale of destruction and unprecedented loss of life following the December 2004 Sumatra tsunami served as the catalyst to refocus efforts in the United States on reducing tsunami vulnerability of coastal communities, and on 20 December 2006, the United States Congress passed the "Tsunami Warning and Education Act" under which education and warning activities were thereafter specified and mandated. A "tsunami forecasting capability based on models and measurements, including tsunami inundation models and maps..." is a central component for the protection of United States coastlines from the threat posed by tsunamis. The forecasting capability for each community described in the PMEL Tsunami Forecast Series is the result of collaboration between the National Oceanic and Atmospheric Administration office of Oceanic and Atmospheric Research, National Weather Service, National Ocean Service, National Environmental Satellite, Data, and Information Service, the University of Washington's Joint Institute for the Study of the Atmosphere and Ocean, National Science Foundation, and United States Geological Survey.

NOAA Center for Tsunami Research

Abstract

This study documents the development of a tsunami forecast model for Arecibo, Puerto Rico. The town of Arecibo is located on the northern coast of the island of Puerto Rico in the Atlantic Ocean. It is particularly exposed to tsunamis originating in the Puerto Rico Trench approximately 100 km north of the island. The Puerto Rico Trench separates the North American and Caribbean plates and extends for approximately 1750 km with a width of almost 100 km. The trench has a maximum depth of 8,648 m, located at Milwaukee Point, the deepest area outside of the Pacific Ocean. Since there is no quantitative information about large historical tsunami events for the island of Puerto Rico, it is not possible to use such events for validation of the inundation forecast model for Arecibo. Accuracy of the results is addressed in this study by comparing the solution obtained using the forecast model with a higher resolution model for 6 synthetic mega-tsunami scenarios originating in the Atlantic Ocean, including the Caribbean Sea. In addition to the mega-tsunami scenarios presented here, a more probable Mw 7.5 scenario is simulated, as well as a micro-tsunami triggered by a seismic event in the South Sandwich Islands, located in the South Atlantic. Results from this study confirm that the Puerto Rico Trench poses the largest tsunami hazard to Arecibo.

Chapter 1

Background and Objectives

The Pacific Marine Environmental Laboratory (PMEL) of the National Oceanic and Atmospheric Administration (NOAA) Center for Tsunami Research (NCTR) has developed a tsunami forecasting capability for operational use by NOAA's two Tsunami Warning Centers located in Hawaii and Alaska (Titov et al., 2005). The system is designed to efficiently provide basin-wide warning of approaching tsunami waves. The system termed Short-term Inundation Forecast of Tsunamis (SIFT) combines real-time tsunami event data with numerical models to produce estimates of tsunami wave arrival times and amplitudes at a coastal community of interest. The SIFT system integrates several key components: deep-ocean, real-time observations of tsunamis, a basin-wide pre-computed propagation database of water level and flow velocities based on potential seismic unit sources, an inversion algorithm to refine the tsunami source based on deep-ocean observations during an event, and optimized tsunami forecast models.

The objective of the present work is to construct a tsunami inundation model for Arecibo, Puerto Rico (see Figure 1), that can be used by the Tsunami Warning Centers to assess, in real time, the local impact of a tsunami generated anywhere in the Atlantic Ocean, particularly in the Caribbean Sea.

The most relevant bathymetric feature offshore of Arecibo is the Puerto Rico Trench (see Figure 2). The trench is the result of the Caribbean and North American plates sliding past each other and is the deepest point in the Atlantic Ocean. It has the potential for triggering large tsunami events, having generated earthquakes with magnitude larger than Mw 8.0 in the past, such as the 1787 Lisbon event. At a more local scale, Arecibo Canyon, a submarine valley located offshore of Arecibo, could behave as a tsunami wave-guide.

This report details the development of a high-resolution tsunami forecast model for Arecibo, including development of the bathymetric grids, model validation and stability testing with a set of synthetic mega-tsunami events (Mw 9.3). Inundation results from such artificial events are presented in later sections.

Chapter 2

Forecast Methodology

A high-resolution inundation model was used as the basis for an operational forecast model to provide an estimate of wave arrival time, height, and inundation immediately following tsunami generation. Tsunami forecast models are run in real time while the tsunami in question is propagating across the open ocean. These models are designed and tested to perform under very stringent time constraints given that time is generally the single limiting factor in saving lives and property. The goal is to maximize the amount of time that an at-risk community has to react to a tsunami threat by providing accurate information quickly.

The tsunami forecast model, based on the Method of Splitting Tsunami (MOST), emerges as the solution in the SIFT system by modeling real-time tsunamis in minutes. SIFT employs high-resolution grids constructed by the National Geophysical Data Center or, in limited instances, internally. Each forecast model consists of three nested grids with increasing spatial and temporal resolution for simulation of wave inundation onto dry land. The forecast model utilizes the most recent bathymetry and topography available to reproduce the correct wave dynamics during the inundation computation. Forecast models are constructed for populous, at-risk communities in the Pacific and Atlantic Oceans. Previous and present development of forecast models in the Pacific (Titov et al., 2005; Titov, 2009; Tang et al., 2009; Wei et al., 2008) have validated the accuracy and efficiency of the forecast models currently implemented in the SIFT system for real-time tsunami forecasting. The model system is also a valuable tool in hindcast research. Tang et al. (2009) provide forecast methodology details.

Chapter 3

Model Development

Modeling of coastal communities is accomplished by developing a set of three nested grids that telescope down from a large spatial extent to a grid that finely defines the bathymetric and topographic features of the community under study. The original bathymetric and topographic grid data used in the development of the Arecibo model were provided by the National Geophysical Data Center (NGDC) under PMEL contract. Details of data gathering and grid construction are provided by Taylor et al. (2007). For each community, data are compiled from a variety of sources to produce a digital elevation model referenced to Mean High Water in the vertical and to the World Geodetic System 1984 in the horizontal (http://ngdc.noaa.gov/mgg/in undation/tsunami/inundation.html). From these digital elevation models, a set of three high-resolution reference models are constructed which are then "optimized" to run in an operationally specified period of time.

The bathymetry and topography used in the development of this forecast model was based on a digital elevation model provided by the NGDC and the author considers it to be an adequate representation of the local topography/bathymetry. As new digital elevation models become available, forecast models will be updated and report updates will be posted at *http://nctr. pmel.noaa.gov/forecast_reports*

3.1   Forecast area

An aerial image of the town of Arecibo can be seen in Figure 1, showing uneven population distribution throughout the study area. The city of Arecibo is nestled between the Rio Grande de Arecibo and Tanamá River on the northern coast of the island of Puerto Rico, approximately 70 km east of the capital city of San Juan. The population is estimated at 95,816 according to the U.S. Census (2011). According to the Fundación Puertoriqueña de las Humanidades: "The fertility of the land in Arecibo favored the development of agriculture, and the principal crop in the first half of the 20th century was sugar cane. Pineapple and other fruits were also planted. Arecibo also had a wealth of livestock ranches. The Arecibo River is known for its freshwater fish. Other sources of income for the municipality are the operation of various manufacturing factories in areas such as distilling and the production of paper, clothing, and chemical products." (source: Fundación Puertoriqueña de las Humanidades, 2014).

3.2 Historical Events and Data

A tide gauge operated by the National Ocean Service (9757809) was deployed on the Arecibo pier (18.48052° N, 66.70236° W) on 5 March 2007. The gauge is located by the breakwater on the northeastern corner of Arecibo Beach, extending southwest from the Arecibo lighthouse. The lower right panel of Figure 3 shows the location of the tide gauge within the inundation grid (grid C) of the forecast model. Table 1 lists the most significant recent near-field events impacting the island of Puerto Rico. Given that there is no tide gauge data for these events, another method must be employed to validate the forecast model. Consequently, validation is based on comparing the high-resolution model results with that of the forecast model.

3.3 Model Setup

Setup of the computational grids for the Method of Splitting Tsunami (MOST) code (Titov and Synolakis, 1998) requires a total of three nested grids for which the outer grid A has the lowest spatial resolution, but covers the largest area, and the inner grid C has the highest spatial resolution, but covers a reduced geographical area. The code makes use of an additional intermediate grid B with medium resolution and spatial coverage. Each interior grid area is completely enclosed by the exterior grid, and inundation is computed only in the most interior grid (Grid C). The purpose of the set of three nested grids is to ensure that as the tsunami wavelength shrinks while traveling from deep to shallow water, the model maintains an approximately constant number of grid nodes per wavelength.

Wave propagation results from a pre-computed ocean wide simulation at lower resolution (4 arc min x 4 arc min) are introduced into this set of three nested grids. The resolution of the ocean-wide propagation grid was selected to adjust numerical dispersion in the code, in order to mimic the effect of physical dispersion (Burwell et al., 2007).

During the development of an operational forecast model, a higher-resolution set of grids, referred to as the reference model, is generated first. The purpose of the reference model is to evaluate grid convergence between a high-resolution model and the forecast model, ensuring that the solution obtained with the lower-resolution forecast model is consistent with that computed with the high-resolution reference model.

Several factors were critical in designing the Arecibo model grids. One is the presence of extensive areas of extremely shallow water around the Caribbean arc. Tsunami waves propagating over these shallow regions will experience a shortening of their wavelength as they approach the island of Puerto Rico. It is important, therefore, to model wave propagation over these areas using a higher resolution grid than that used for the simulations stored in the deep-water propagation database (4-arc-min resolution). This is accomplished in the present model by extending the outermost grid of the three nested grids (Grid A) to the east and south of Puerto Rico. The resolution of Grid A in the present model is 47.24 arc sec in the zonal direction and 4 arc sec in the meridional direction, permitting the resolution of much higher frequency waves over shallow regions than the 4-arc-min propagation database grid.

In addition, the A grid used in the current forecast model is identical to that used in other Caribbean region forecast models, such as the Charlotte Amalie, U.S. Virgin Islands. This setup is potentially advantageous in future configurations of SIFT software, making it possible to compute the A grid only once and to share the computation results with all forecast models

located within the geographical extent of the grid, avoiding multiple computations of the same grid for different forecast models.

The local topography was also considered in the design of the Arecibo forcast model grids. The surrounding area of Arecibo includes some low-lying coastal plains susceptible to inundation. The southern boundary of the model's inundation grid (Grid C) was located far enough inland so as to include most of the coastal plain in the grid. This configuration will ensure that even in the worst case scenario, tsunami runup will not exceed the grid boundaries.

The location of a densely populated coastal area mostly to the west of the tide gauge location was also a consideration when determining the location of the western boundary of the grid. Figure 3 highlights the difference between the reference and the forecast model grids and Figures 4 and 5 show grid coverage area and relative grid position with respect to the community and local bathymetric features for the reference and forecast models, respectively. Table 2 summarizes the parameters and model setup for each set of grids.

Chapter 4

Results and Discussion

Three types of tests are typically performed to assess forecast model convergence, accuracy and robustness. However, in the case of Arecibo, since no historical data are available, accuracy tests based on historical events could not be performed.

To assess model convergence, results obtained with the reference model were compared with those obtained with the forecast model to confirm consistency of results at least for the leading tsunami waves. This type of test is not, strictly speaking, a grid convergence test in the sense used in computational science, since the solution is compared on grids with varying resolution, coverage and bathymetric information; however, it provides a good estimate of the similarities and discrepancies between the solution of a more accurate, high-resolution model of the area and that of a lower-resolution, run-time optimized forecast model.

Robustness tests include the simulation of 6 tsunamis generated by Mw 9.3 earthquakes throughout the Caribbean and Atlantic basin, a medium magnitude event (Mw 7.5) and a small magnitude (micro-tsunami, Mw 6.2) event. Figure 6 shows the epicenter locations of these artificial events. Forecast model simulations proved to be free of instabilities during 24 hours of simulation for each of these synthetic mega- and micro-events.

During the development of the present forecast model, a west-travelling wave from the eastern boundary of the coastal lagoon (right edge of Grid C) was observed while examining the animations of events with local co-seismic deformation in Arecibo. This is most likely caused by the current operational version of MOST modifying the local bathymetry in the case of local seismic deformation, but leaving the topography unchanged. Grid nodes interior to the coastal lagoon are considered bathymetric nodes (wet points) and experience subsidence during a local event. MOST applies the computed subsidence to these grid nodes, effectively lowering the water level in the lagoon below sea level. On the eastern boundary of the coastal lagoon (eastern edge of Grid C) wave values are interpolated from nearby exterior nodes in Grid B. Some of those nodal values correspond to land values with 0 wave elevation. Consequently, the wave height value along the eastern boundary of the lagoon is the average of some neighboring wet points (lagoon wet points in Grid B) and some dry points that fall outside of the lagoon in Grid B. The wet points have subsided below sea level due to the seismic deformation by the same amount as the lagoon wet points in Grid C. Therefore, at these nodes, wave height values will be negative. The dry points, however, maintain a wave height value of 0. MOST will then perform bilinear interpolation to compute new wave elevation values in nodes located along the eastern boundary of Grid C. These interpolated wave height values will be higher than the subsided water elevation of the lagoon. The difference in wave height causes a perturbation on the

surface of the lagoon that manifests itself as left-traveling wave. A good indication that this assumption is correct is the fact that, when the MOST code was modified so that no bathymetric co-seismic deformation was applied to the coastal lagoon, no left-traveling wave appeared in the lagoon.

4.1   Model Validation

As there are no recorded historical cases for Arecibo, the validity of the forecast model was assessed by comparing the forecast model solution with that obtained using the high-resolution model for 8 synthetic scenarios. Since most of the tested scenarios are Mw 9.3, this set of tests was also used to establish the stability of the forecast model.

4.2   Model Stability Testing Using Synthetic Scenarios

During model stability testing, 8 synthetic tsunamis (earthquake Mw 9.3, Mw 7.5, and Mw 6.2) were simulated using the forecast model. Details of the 8 synthetic events tested can be found in Table 3. Each of the six extreme synthetic mega-events is constructed along a 1000-km-long and 100-km wide fault plane with a uniform slip amount of 25 m along the fault. The output from the code at every time step was visualized and inspected for instabilities. The cause of any instability was corrected and a final set of forecast grids emerged from the process. Most of the forecast model instabilities were associated with deficient resolution to distinguish small bathymetric and topographic features.

Six of the eight synthetic events used as test cases in this study were generated by earthquakes with epicenters located at different points along the Caribbean Island Arc. The microtsunami event (Mw 6.2) was designed to be generated by a far-field earthquake in the South Sandwich Islands. Time series comparison of the results obtained with the high-resolution model and with the forecast model show very good agreement, with almost a one to one comparison during the first hour of simulation for all cases as evidenced in Figures 7 through 14. However, any differences between the high-resolution and forecast models during the first hour of simulation were characterized by discrepancies in the maximum amplitude of the wave train between both simulations. Some of the simulations (e.g., Synthetic Scenarios 4 and 6) show excellent comparison between the two models even 10 hr into the simulation.

Of all six mega-tsunami events tested, Synthetic Scenario 2 poses the greatest tsunami hazard to Arecibo with predicted wave amplitude of almost 15 m at the Arecibo tide gauge. This is hardly surprising since Synthetic Scenario 2 represents a Mw 9.3 tsunami event generated in the Puerto Rico Trench, directly offshore of the coast of Arecibo. Of all cases tested during the present study, this is undoubtedly the worst case scenario for Arecibo as evidenced in Figures D1 and D2 in Appendix D. Synthetic Scenario 2 is also the worst case scenario for the eastern seaboard of the United States. However, this scenario was designed merely to test the stability and performance of the forecast model during a very large local event. The credibility of such a scenario as a viable earthquake event at that location has not been taken into consideration. Consequently these results should not be interpreted as a tsunami hazard study for Arecibo or the East Coast of the United States, but as numerical exercises to test the computational stability of the forecast model.

Additional cases generating a certain amount of inundation at Arecibo are Synthetic Scenarios 1 and 5, with tsunamis originating along the eastern segment of the Caribbean Island Arc and off of the Caribbean coastline of Honduras, respectively. Figures 15 through 22 show the comparison between the inundation extents and maximum wave amplitudes for all 8 synthetic scenarios computed with the reference and forecast models.

Chapter 5

Summary and Conclusions

A set of tsunami forecast grids has been developed for operational use by the Tsunami Warning Centers in conjunction with the Method of Splitting Tsunami code. Two sets of grids were developed: a high-resolution set intended to provide reference values, and a forecast set designed to minimize processor run time and to provide real-time tsunami estimates in Arecibo, Puerto Rico.

The presence of some geographical features unique to the area were decisive in the design of the forecast model grids for Arecibo. The two most relevant features were the presence of very extensive shallow areas along the Caribbean Island Arc and the existence of a shallow-water coastal lagoon in the town of Arecibo.

The standard procedure of testing the accuracy of the model with data from historical events and evaluating computed results with observations could not be performed in this case due to the lack of good quantitative data for recent historical tsunami events in the area. Therefore, the accuracy and stability of the forecast model had to be evaluated by comparing forecasted results of a series of mega-tsunami events with results obtained on a set of higher-resolution grids.

Even though the synthetic events used to perform stability tests on the forecast model may not necessarily represent credible seismic scenarios, the directivity of their tsunamis can be interpreted as an indicator of what parts of the Caribbean pose the greatest tsunami hazard for Arecibo. In this respect, the results of our simulations show that an event in the Puerto Rico Trench immediately offshore of Arecibo represents the worst case scenario, followed by events from the East and West boundaries of the Caribbean Island Arc.

Even though the design of the forecast model grids includes a high-resolution representation of the shallow water areas along the Caribbean Island Arc in Grid A, this had minor impact on processor run time. The forecast model was still capable of simulating 4 hrs of tsunami activity in 11.35 min of wall clock time on an Intel Xeon E5670 2.3 processor.

Chapter 6

Acknowledgments

Chapter 7

References

Burwell, D., E. Tolkova and A. Chawala (2007). Diffusion and dispersion characterization of a numerical tsunami model. *Ocean Modelling*, Vol. 19, Issues 1-2, ISSN 1463-5003.52

Fundación Puertoriqueña de las Humanidades. http://www.enciclopediapr.org/ing/article.cfm?ref=09022301&page=2). Accessed: 15 March 2012

Tang, L., V.V. Titov and C.D. Chamberlin (2009). Development, testing, and applications of site-specific tsunami inundation models for real-time forecasting. *J. Geophys. Res*, Vol.114, C12025, doi: 10.1029/2009JC005476, ISSN 1463-5003.52.

Titov, V.V. and C.E. Synolakis (1998). Numerical modeling of tidal wave runup. *J. Waterw. Port Coast. Ocean Eng*, 124(4), 157-171.

Titov, V.V., F.I. González, E.N. Bernard, M.C. Eble, H.O. Mofjeld, J.C. Newman and A.J. Venturato (2005). Real-time tsunami forecasting: Challenges and solutions. *Nat. Hazards.*, 35(1), 41-58.

Titov, V.V. (2009). Tsunami forecasting. In *The Sea*, Vol. 15, Chapter 12, Harvard University Press, Cambridge, MA and London, England, 371-400.

Taylor, L.A., B.W. Eakins, K.S. Carignan, R.R. Warnken, T. Sazonova and D.C. Schoolcraft. (2007). Digital Elevation Models for Puerto Rico: Procedures, Data Sources and Analysis. National Geophysical Data Center. June 22 2007.

Wei, Y., E. Bernard, L. Tang, R. Weiss, V. Titov, C. Moore, M. Spillane, M. Hopkins and U. Kânoğlu. (2008). Real-time experimental forecast of the Peruvian tsunami of August 2007 for U.S. coastlines. *Geophys. Res. Lett.*, L04609, doi: 10.1029/2007GL032250.

U.S. Census. http://factfinder2.census.gov/faces/nav/jsf/pages/community_facts.xhtml#none. Accessed: 28 April 2014

U.S. Geological Survey. Earthquake and Tsunamis in PR and the U.S. VI. http://pubs.usgs.gov/fs/fs141-00/fs141-00.pdf. Accessed: 28 April 2014

FIGURES

Figure 1: Aerial view of the Port of Arecibo showing the beach and the pier to the right of the image. The mouth of the Rio Grande de Arecibo and population center is to the left (courtesy of Google Maps).
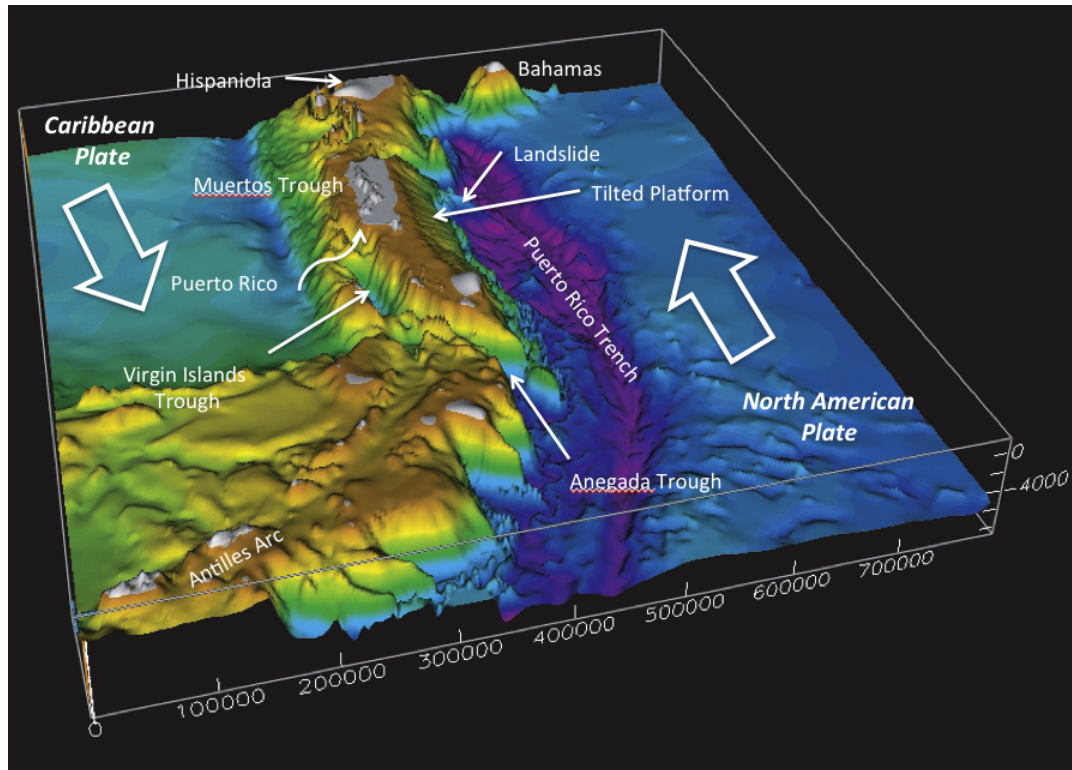
Figure 2: Schematic of tectonic motion and location of major bathymetric features in the vicinity of Puerto Rico (from USGS Science for a Changing World, Earthquake and Tsunamis in Puerto Rico and the U.S. Virgin Islands).
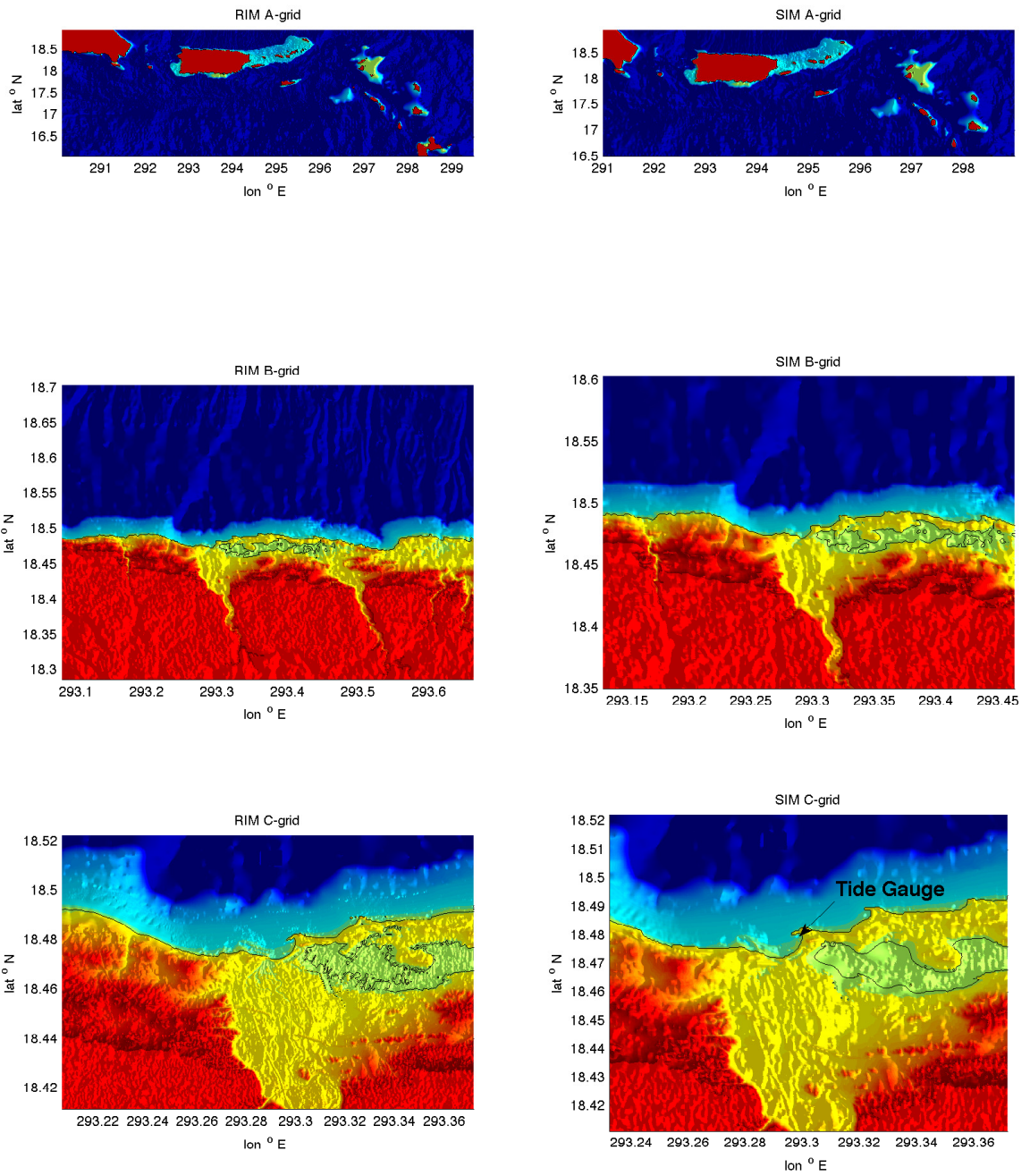
Figure 3: Comparison between the reference and forecast model grids. The location of the Arecibo tide gauge on the south side of the pier is indicated in the lower right panel.
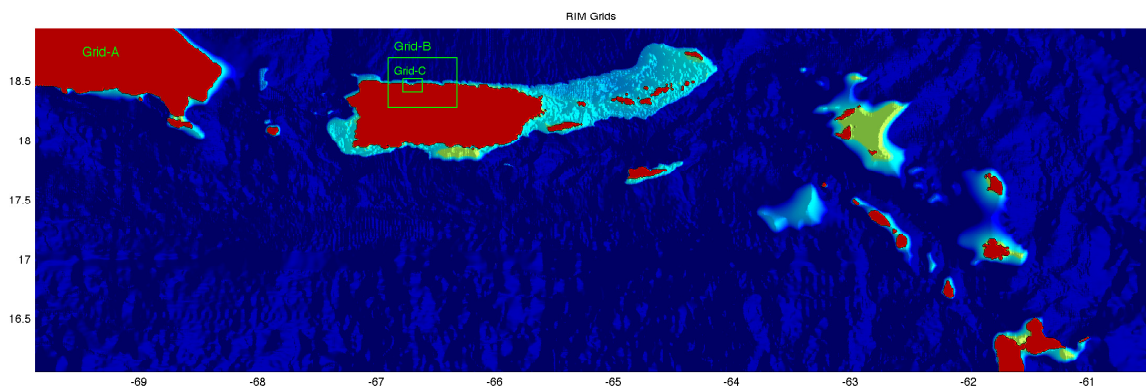
Figure 4: Map of the Northeastern Caribbean arc showing the position of the reference model grids relative to Arecibo and the island of Puerto Rico

Grid-A

Grid-B
Grid-C
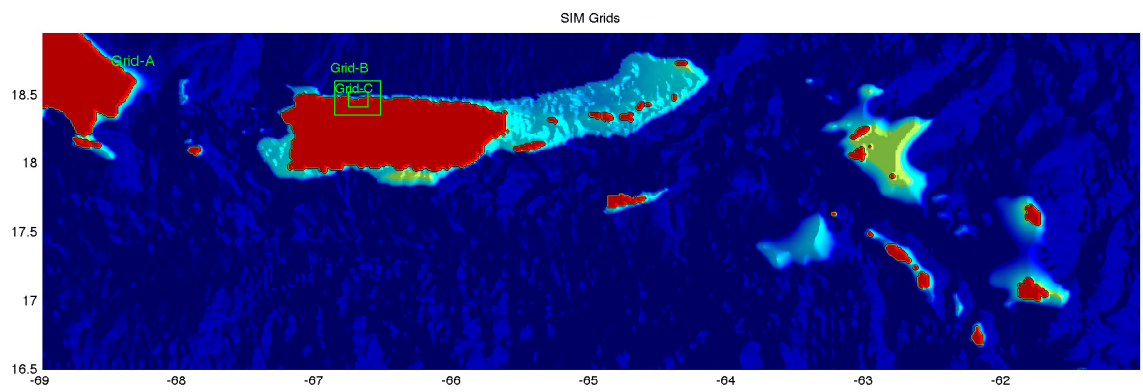
Figure 5: Map of the Northeastern Caribbean arc showing the position of the forecast model grids relative to Arecibo and the island of Puerto Rico.
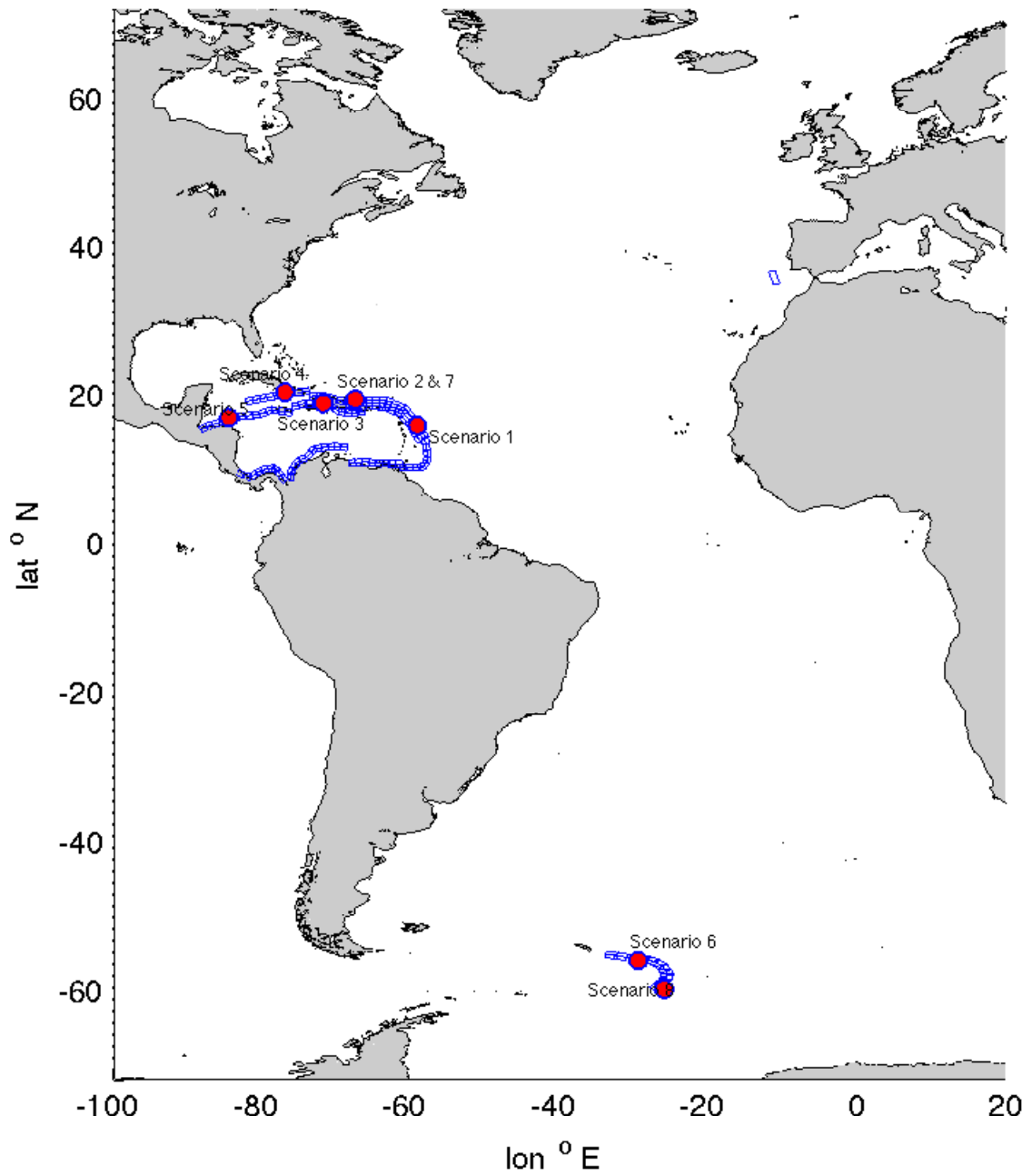
Figure 6: Location of the mid-rupture point of 8 synthetic (Mw 9.3) events used in the model robustness tests, showing the relative position of Puerto Rico to the epicenter locations.
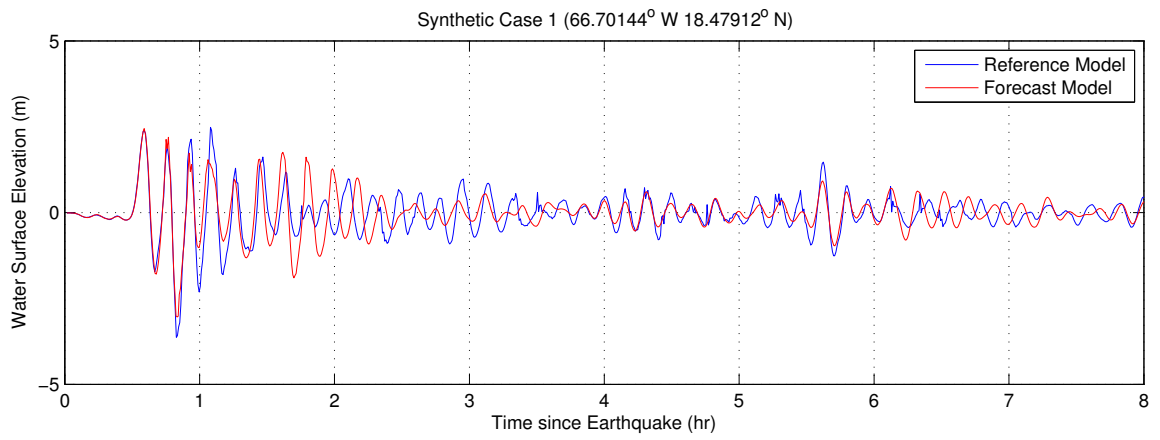
Figure 7: Comparison of the forecast and reference models for Synthetic Scenario 1.
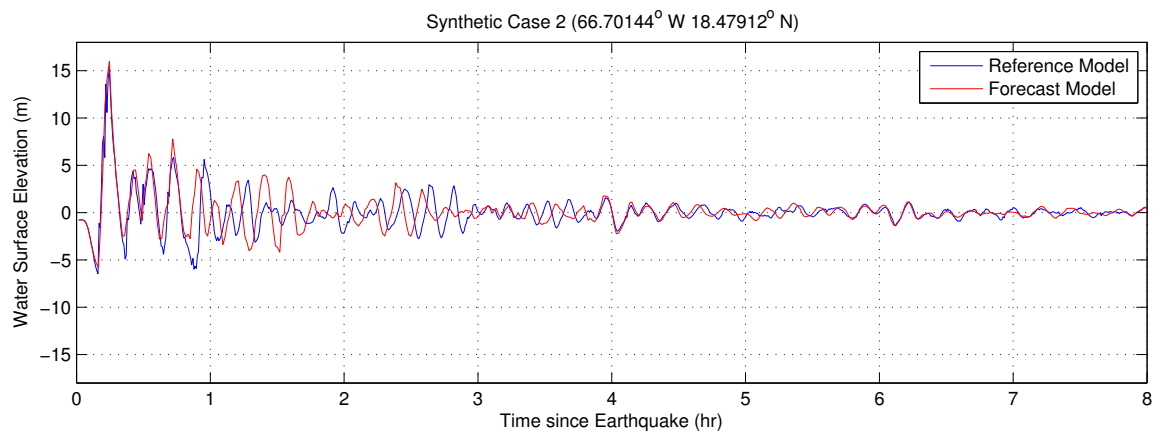
Figure 8: Comparison of the forecast and reference models for Synthetic Scenario 2.
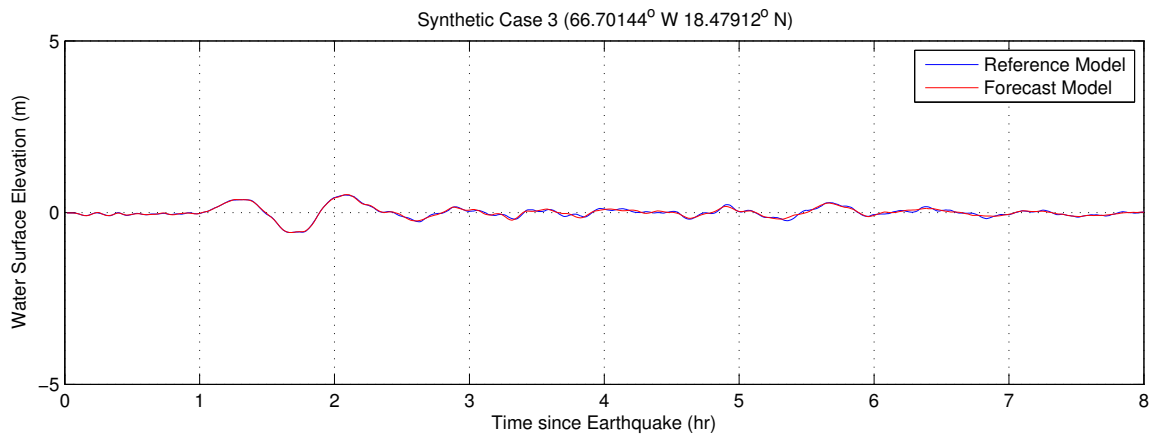
Figure 9: Comparison of the forecast and reference models for Synthetic Scenario 3.
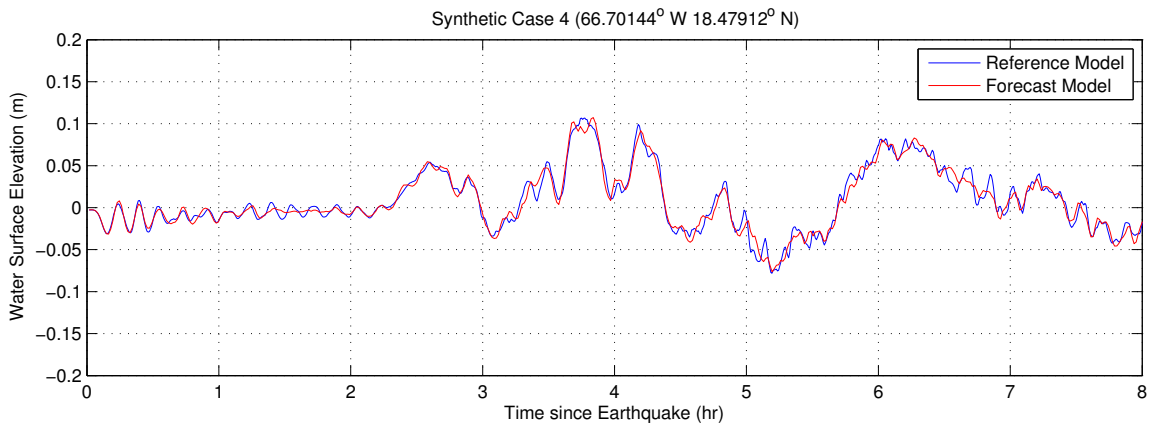
Figure 10: Comparison of the forecast and reference models for Synthetic Scenario 4.

Synthetic Case 5 (66.70144° W 18.47912° N)
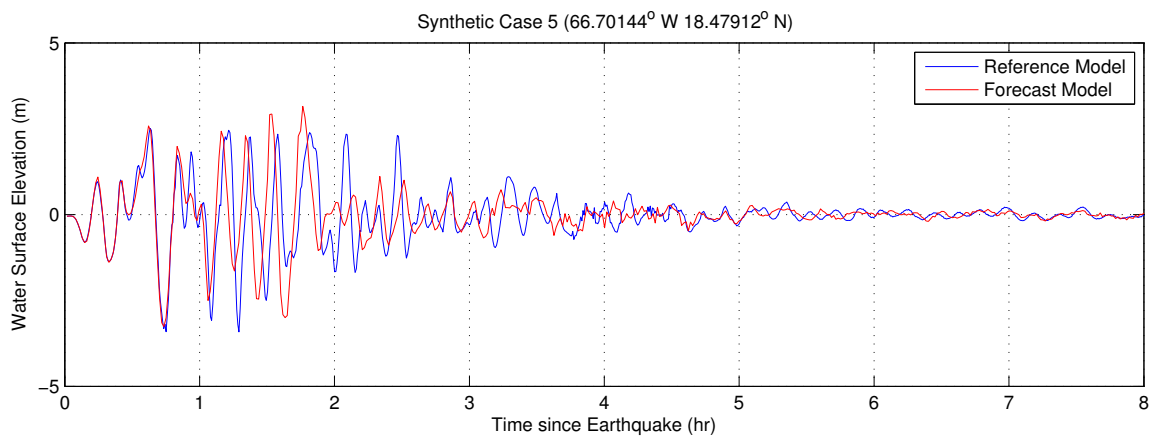
Figure 11: Comparison of the forecast and reference models for Synthetic Scenario 5.
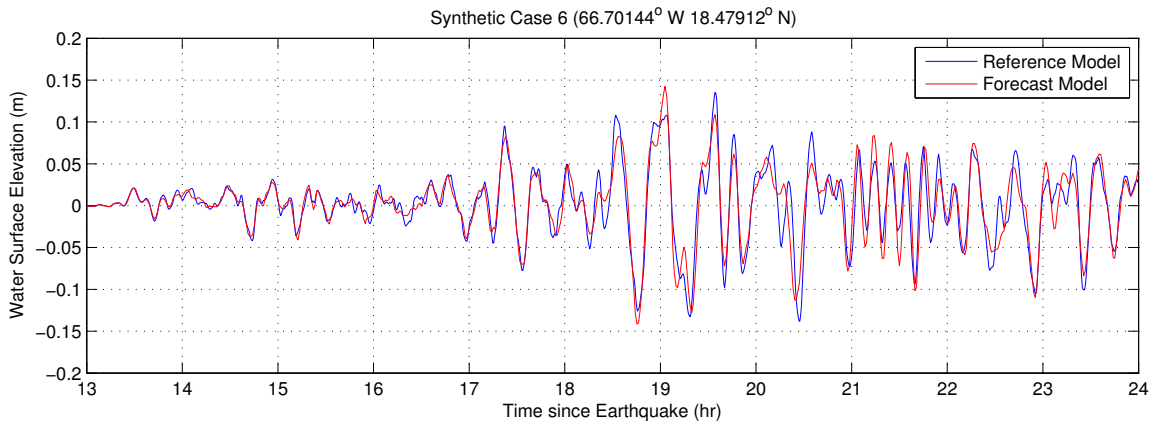
Figure 12: Comparison of the forecast and reference models for Synthetic Scenario 6.
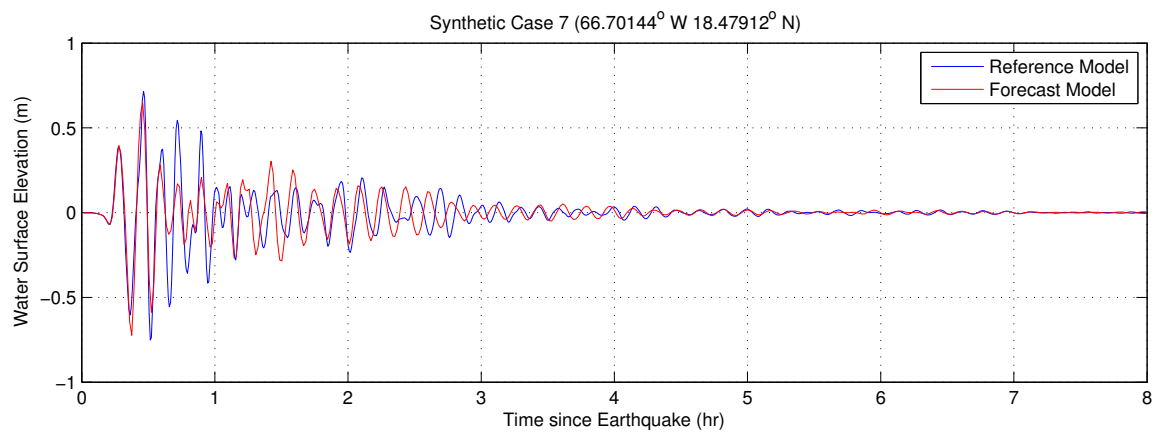
Figure 13: Comparison of the forecast and reference models for Synthetic Scenario 7.
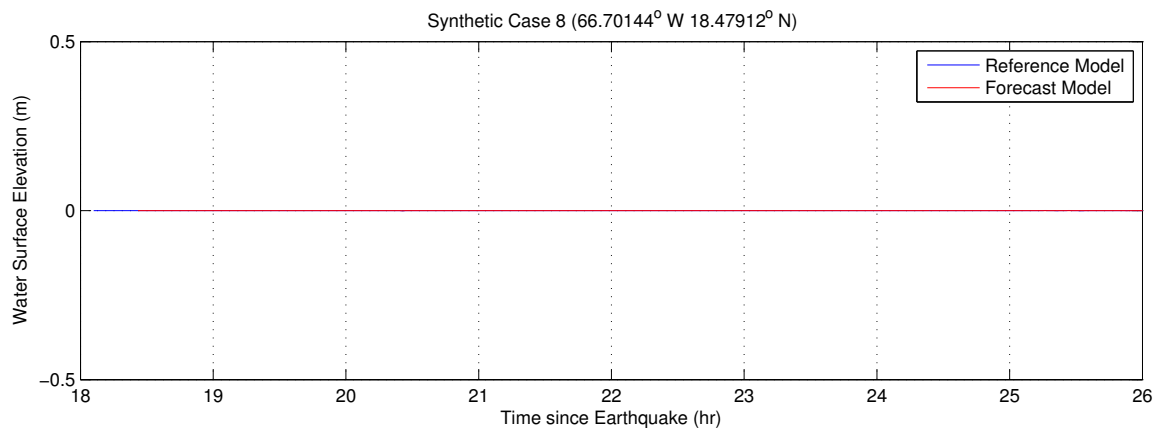
Figure 14: Comparison of the forecast and reference models for Synthetic Scenario 8.

Synthetic Case 1
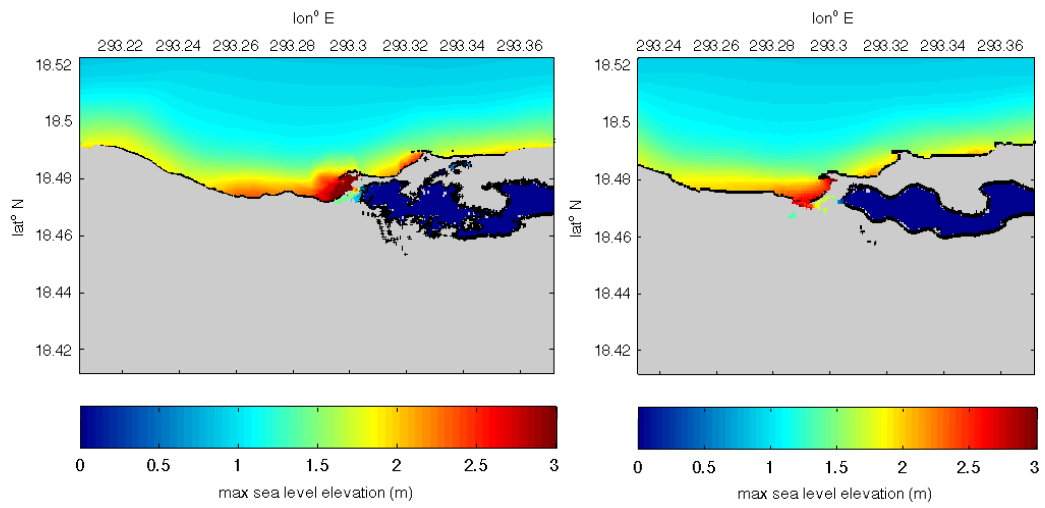
Figure 15: Maximum sea surface elevation computed with the reference (left) and forecast (right) models for Synthetic Scenario 1.
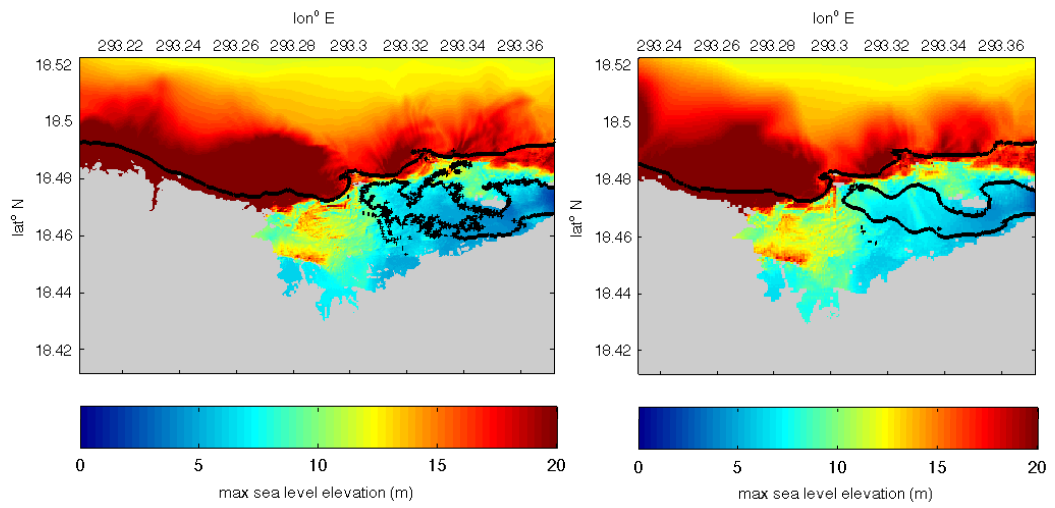
Figure 16: Maximum sea surface elevation computed with the reference (left) and forecast (right) models for Synthetic Scenario 2.
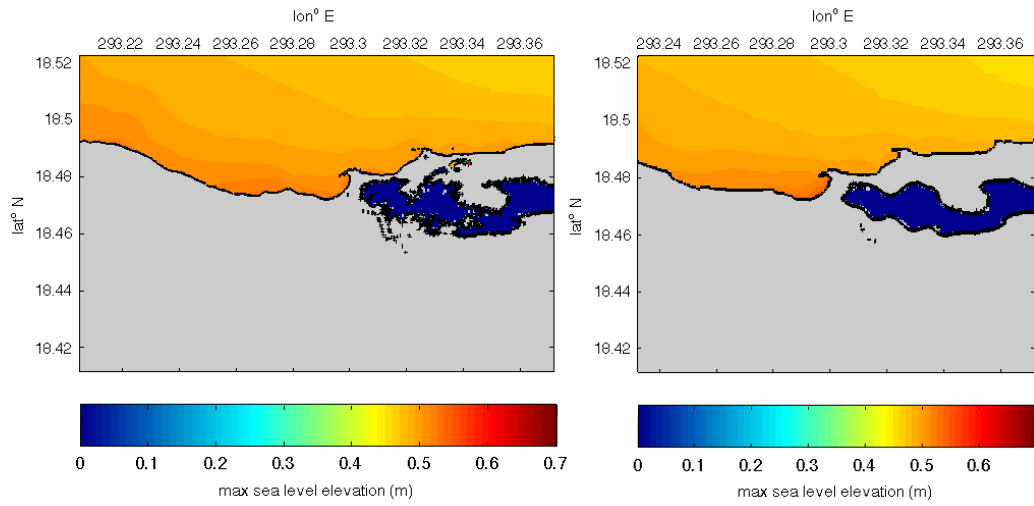
Figure 17: Maximum sea surface elevation computed with the reference (left) and forecast (right) models for Synthetic Scenario 3.
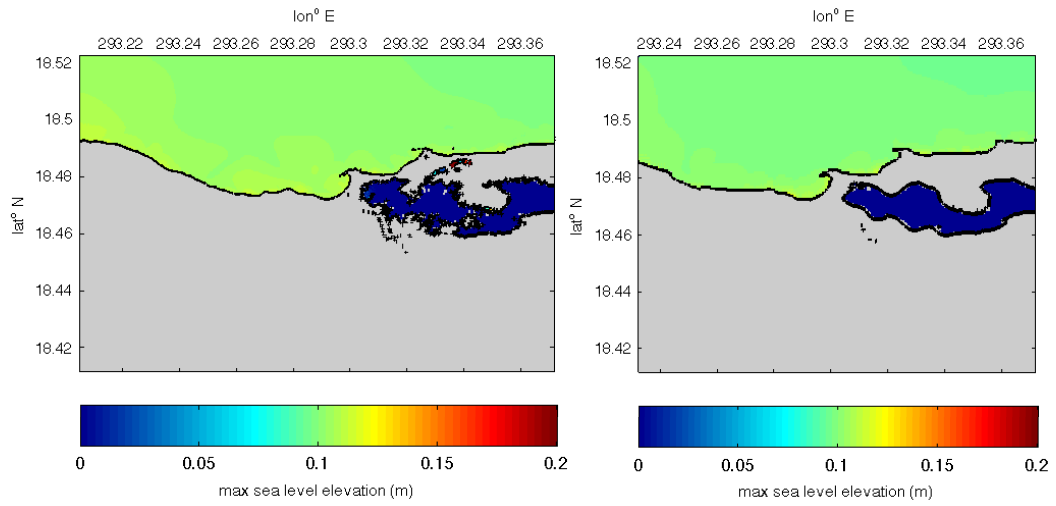
Figure 18: Maximum sea surface elevation computed with the reference (left) and forecast (right) models for Synthetic Scenario 4.

Figure 19: Maximum sea surface elevation computed with the reference (left) and forecast (right) models for Synthetic Scenario 5.

Synthetic Case 6.
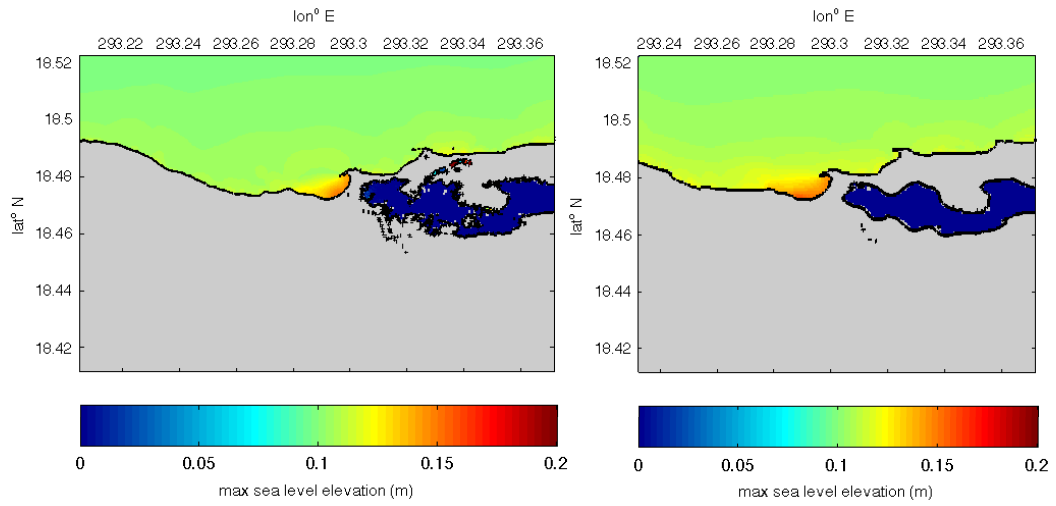
Figure 20: Maximum sea surface elevation computed with the reference (left) and forecast (right) models for Synthetic Scenario 6.

Synthetic Case 7.
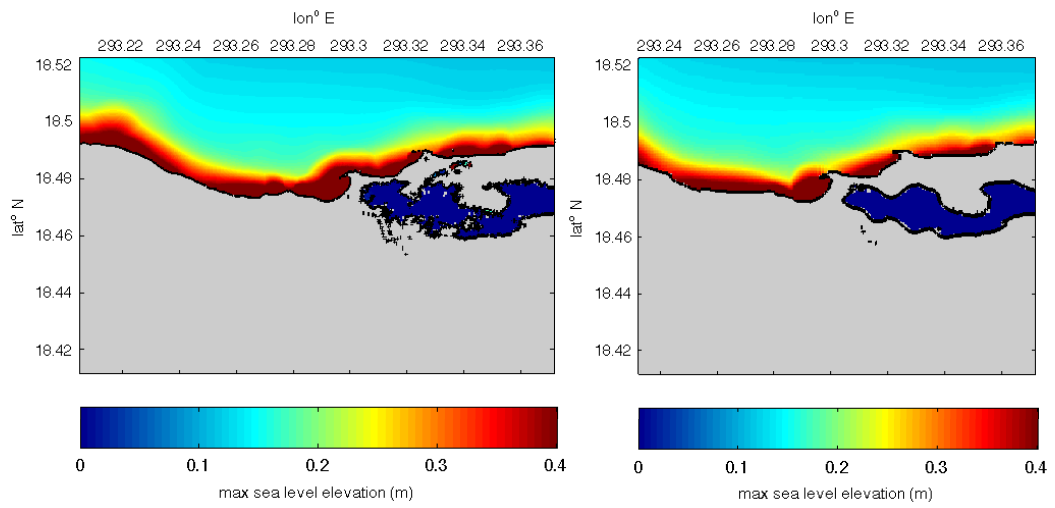
Figure 21: Maximum sea surface elevation computed with the reference (left) and forecast (right) models for Synthetic Scenario 7.
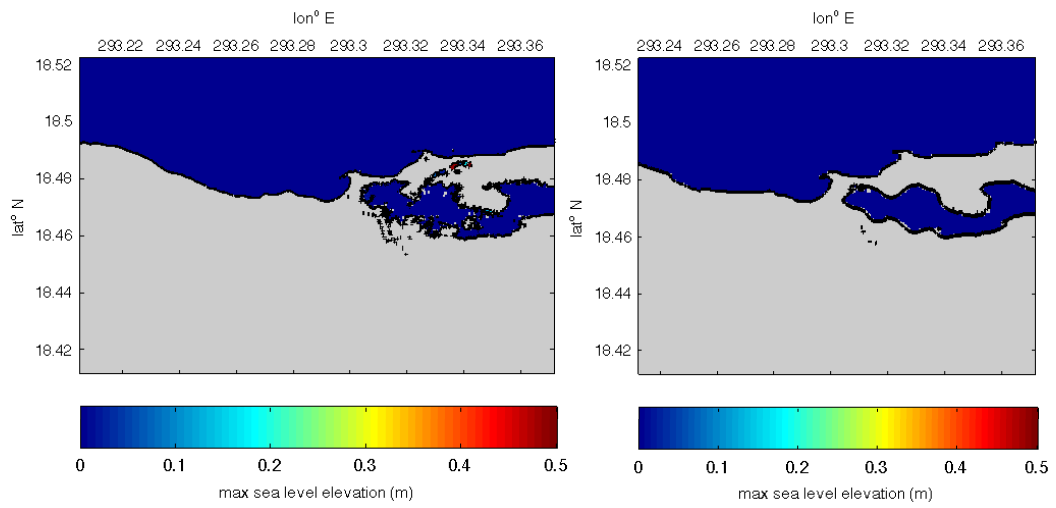
Figure 22: Maximum sea surface elevation computed with the reference (left) and forecast (right) models for Synthetic Scenario 8.

TABLES

Earthquake location	Date	Magnitude
Hispaniola	1953	6.9
Mona Canyon	1946	7.5
Hispaniola	1946	8.1
Mona Canyon	1918	7.5
Anegada Trough	1867	7.5
Puerto Rico Trench	1787	8.1

Table 1: Most significant earthquakes in the Puerto Rico area in the last 3 centuries.

Model Setup	Reference Model				Forecast Model		
	Grid A	Grid B	Grid C		Grid A	Grid B	Grid C
W	W69.90	W66.92	W66.80		W69.00	W66.87	W66.775
E	W60.50	W66.34	W66.63		W61.00	W66.53	W66.281
S	N18.95	N18.70	N18.52		N18.95	N18.60	N18.522
N	N16.05	N18.28	N18.41		N16.50	N18.35	N18.411
dx	20.97"	6"	1"		47.24"	6"	2"
dy	20"	6"	1"		45"	6"	2"
$nx \times ny$	1614×523	351x251	601×401		610×197	201x153	252×201
dt (sec)	2.3	1.23	1.00		5.2	1.58	0.78
D_{min}	1 m				1 m		
Fric. (n^2)	0.0009				0.0009		
CPU Time	~ 114.76 min for 4-hour simulation				~ 11.35 min for 4-hour simulation		
Warning Pt.	W66.70144, N18.47912						

Table 2: MOST setup parameters for reference and forecast models for Arecibo..

SceNo.	Scenario Name	Source Zone	Tsunami Source	α (m)	Max (m)	Min (m)
		Mega-tsunami scenario				
1	ATSZ 38-47	Atlantic	A38-A47, B38-B47	25	2.52	-3.38
2	ATSZ 48-57	Atlantic	A48-A57, B48-B57	25	14.3	-5.83
3	ATSZ 58-67	Atlantic	A58-A67, B58-B67	25	0.52	-0.59
4	ATSZ 68-77	Atlantic	A68-A77, B68-B77	25	0.11	-0.09
5	ATSZ 82-91	Atlantic	A82-A91, B82-B91	25	3.17	-3.29
6	SSSZ 1-10	South Sandwich	A1-A10, B1-B10	25	0.14	-0.14
		Mw 7.5 Tsunami scenario				
7	ATSZ B52	Atlantic	B52	1	0.10	-0.16
		Micro-tsunami scenario (select one)				
8	SSSZ B11	South Sandwich	B11	0.01	0.0002	-0.0003

Table 3: Synthetic tsunami sources used in the forecast model stability test for Arecibo showing tide gauge maximum and minimum water level elevations.

Appendix A

Development of the Arecibo, Puerto Rico, tsunami forecast model occurred prior to parameter changes that were made to reflect modifications to the MOST model code. As a result, the input file for running both the tsunami forecast model and the high-resolution reference inundation model in MOST have been updated accordingly. Appendix A1 and A2 provide the updated files for Arecibo.

A.1 Reference model ⋆.in file for Arecibo, Puerto Rico

0.0001 Minimum amplitude of input offshore wave (m)
1 Input minimum depth for offshore (m)
0.1 Input "dry land" depth for inundation (m)
0.0009 Input friction coefficient (n ⋆⋆2)
1 let a and b run up
300.0 max eta before blow up (m)
0.38 Input time step (sec)
114000 Input number of steps
5 Compute "A" arrays every nth time step, n=
2 Compute "B" arrays every nth time step, n=
80 Input number of steps between snapshots
1 ...Starting from
1 ...Saving grid every nth node, n=?
bathy/Anew20s_1nd_SSL1.9sm.asc1
bathy/GridB_RIM.crr.ssl
bathy/GridC_RIM.crr.ssl.flt.snk3
../SRCS/Arecibo_srcs/
./rsyn01_run2d/
1 1 1 1
1
3 333 155

A.2 Forecast model ⋆.in file for Arecibo, Puerto Rico

0.0001 Minimum amplitude of input offshore wave (m)
1 Input minimum depth for offshore (m)
0.1 Input "dry land" depth for inundation (m)
0.0009 Input friction coefficient (n ⋆⋆ 2)
1 let a and b runup
300.0 max eta before blow up (m)
0.7 Input time step (sec)
41300 Input number of steps
6 Compute "A" arrays every nth time step, n=
2 Compute "B" arrays every nth time step, n=
84 Input number of steps between snapshots
1 ...Starting from
1 ...Saving grid every nth node, n=?
arecibo_run2d/A5_45s_1nd_SSL1.9.asc
arecibo_run2d/GridB_SIM.crr.ssl2
arecibo_run2d/GridC_SIM.crr.ssl.flt.snk.ssl.9.crp2
./
./
1 1 1 1 NetCDF output for A, B, C, SIFT
1 Timeseries locations:
3 118 78

Appendix B

Propagation Database:
Atlantic Ocean Unit Sources

NOAA Propagation Database presented in this section is the representation of the database as of March 2013. This database may have been updated since March 2013.
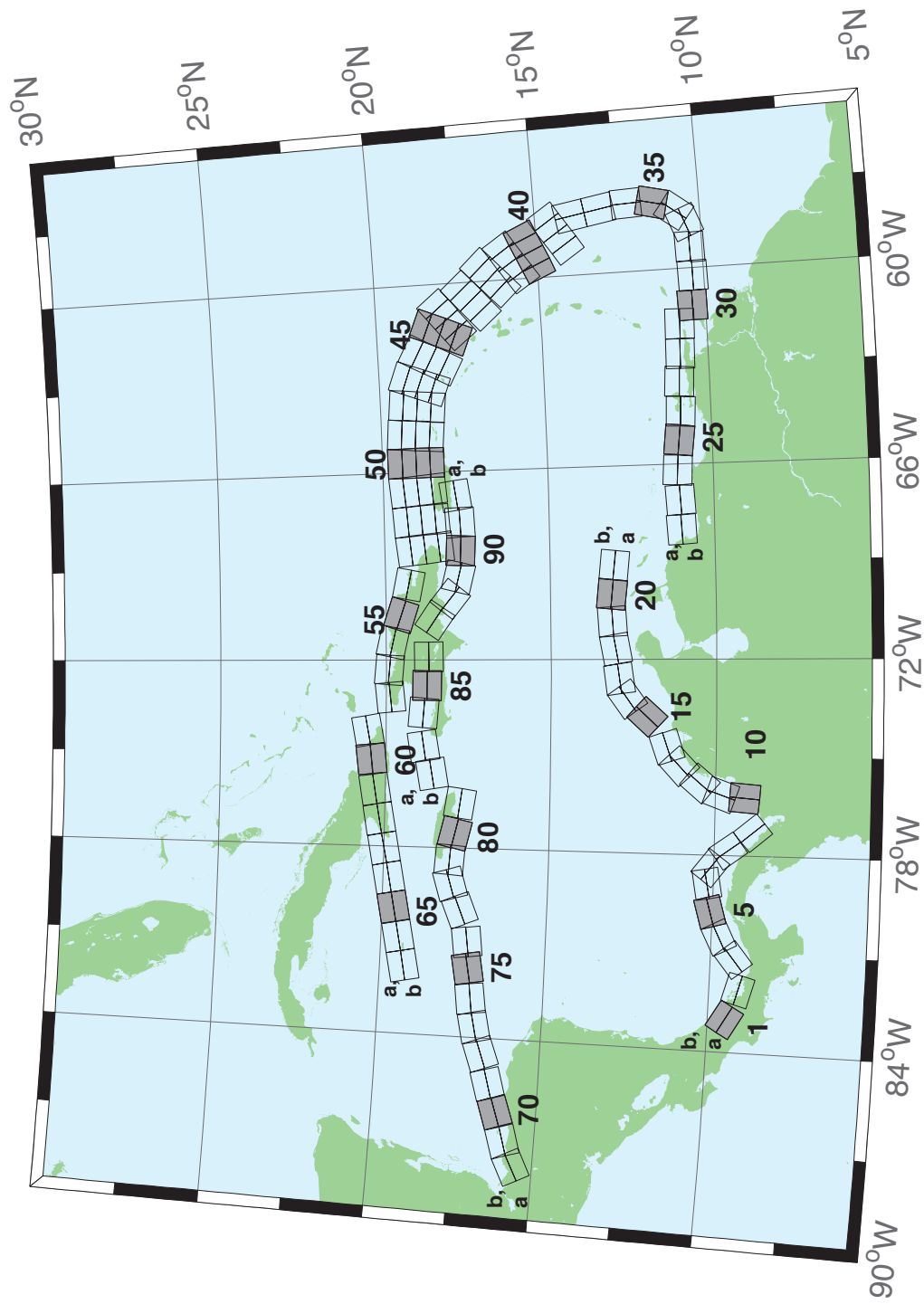
Figure B.1: Atlantic Source Zone unit sources.

Table B.1: Earthquake parameters for Atlantic Source Zone unit sources.

Segment	Description	Longitude(^{o}E)	Latitude(^{o}N)	Strike(^{o})	Dip(^{o})	Depth (km)
atsz–1a	Atlantic Source Zone	-83.2020	9.1449	120	27.5	28.09
atsz–1b	Atlantic Source Zone	-83.0000	9.4899	120	27.5	5
atsz–2a	Atlantic Source Zone	-82.1932	8.7408	105.1	27.5	28.09
atsz–2b	Atlantic Source Zone	-82.0880	9.1254	105.1	27.5	5
atsz–3a	Atlantic Source Zone	-80.9172	9.0103	51.31	30	30
atsz–3b	Atlantic Source Zone	-81.1636	9.3139	51.31	30	5
atsz–4a	Atlantic Source Zone	-80.3265	9.4308	63.49	30	30
atsz–4b	Atlantic Source Zone	-80.5027	9.7789	63.49	30	5
atsz–5a	Atlantic Source Zone	-79.6247	9.6961	74.44	30	30
atsz–5b	Atlantic Source Zone	-79.7307	10.0708	74.44	30	5
atsz–6a	Atlantic Source Zone	-78.8069	9.8083	79.71	30	30
atsz–6b	Atlantic Source Zone	-78.8775	10.1910	79.71	30	5
atsz–7a	Atlantic Source Zone	-78.6237	9.7963	127.2	30	30
atsz–7b	Atlantic Source Zone	-78.3845	10.1059	127.2	30	5
atsz–8a	Atlantic Source Zone	-78.1693	9.3544	143.8	30	30
atsz–8b	Atlantic Source Zone	-77.8511	9.5844	143.8	30	5
atsz–9a	Atlantic Source Zone	-77.5913	8.5989	139.9	30	30
atsz–9b	Atlantic Source Zone	-77.2900	8.8493	139.9	30	5
atsz–10a	Atlantic Source Zone	-75.8109	9.0881	4.67	17	19.62
atsz–10b	Atlantic Source Zone	-76.2445	9.1231	4.67	17	5
atsz–11a	Atlantic Source Zone	-75.7406	9.6929	19.67	17	19.62
atsz–11b	Atlantic Source Zone	-76.1511	9.8375	19.67	17	5
atsz–12a	Atlantic Source Zone	-75.4763	10.2042	40.4	17	19.62
atsz–12b	Atlantic Source Zone	-75.8089	10.4826	40.4	17	5
atsz–13a	Atlantic Source Zone	-74.9914	10.7914	47.17	17	19.62
atsz–13b	Atlantic Source Zone	-75.2890	11.1064	47.17	17	5
atsz–14a	Atlantic Source Zone	-74.5666	11.0708	71.68	17	19.62
atsz–14b	Atlantic Source Zone	-74.7043	11.4786	71.68	17	5
atsz–15a	Atlantic Source Zone	-73.4576	11.8012	42.69	17	19.62
atsz–15b	Atlantic Source Zone	-73.7805	12.0924	42.69	17	5
atsz–16a	Atlantic Source Zone	-72.9788	12.3365	54.75	17	19.62
atsz–16b	Atlantic Source Zone	-73.2329	12.6873	54.75	17	5
atsz–17a	Atlantic Source Zone	-72.5454	12.5061	81.96	17	19.62
atsz–17b	Atlantic Source Zone	-72.6071	12.9314	81.96	17	5
atsz–18a	Atlantic Source Zone	-71.6045	12.6174	79.63	17	19.62
atsz–18b	Atlantic Source Zone	-71.6839	13.0399	79.63	17	5
atsz–19a	Atlantic Source Zone	-70.7970	12.7078	86.32	17	19.62
atsz–19b	Atlantic Source Zone	-70.8253	13.1364	86.32	17	5
atsz–20a	Atlantic Source Zone	-70.0246	12.7185	95.94	17	19.62
atsz–20b	Atlantic Source Zone	-69.9789	13.1457	95.94	17	5
atsz–21a	Atlantic Source Zone	-69.1244	12.6320	95.94	17	19.62
atsz–21b	Atlantic Source Zone	-69.0788	13.0592	95.94	17	5
atsz–22a	Atlantic Source Zone	-68.0338	11.4286	266.9	15	17.94
atsz–22b	Atlantic Source Zone	-68.0102	10.9954	266.9	15	5
atsz–23a	Atlantic Source Zone	-67.1246	11.4487	266.9	15	17.94
atsz–23b	Atlantic Source Zone	-67.1010	11.0155	266.9	15	5
atsz–24a	Atlantic Source Zone	-66.1656	11.5055	273.3	15	17.94
atsz–24b	Atlantic Source Zone	-66.1911	11.0724	273.3	15	5
atsz–25a	Atlantic Source Zone	-65.2126	11.4246	276.4	15	17.94
atsz–25b	Atlantic Source Zone	-65.2616	10.9934	276.4	15	5
atsz–26a	Atlantic Source Zone	-64.3641	11.3516	272.9	15	17.94
atsz–26b	Atlantic Source Zone	-64.3862	10.9183	272.9	15	5
atsz–27a	Atlantic Source Zone	-63.4472	11.3516	272.9	15	17.94
atsz–27b	Atlantic Source Zone	-63.4698	10.9183	272.9	15	5
atsz–28a	Atlantic Source Zone	-62.6104	11.2831	271.1	15	17.94
atsz–28b	Atlantic Source Zone	-62.6189	10.8493	271.1	15	5
atsz–29a	Atlantic Source Zone	-61.6826	11.2518	271.6	15	17.94
atsz–29b	Atlantic Source Zone	-61.6947	10.8181	271.6	15	5
atsz–30a	Atlantic Source Zone	-61.1569	10.8303	269	15	17.94
atsz–30b	Atlantic Source Zone	-61.1493	10.3965	269	15	5
atsz–31a	Atlantic Source Zone	-60.2529	10.7739	269	15	17.94

44

Segment	Description	Longitude(^{o}E)	Latitude(^{o}N)	Strike(^{o})	Dip(^{o})	Depth (km)
atsz–31b	Atlantic Source Zone	-60.2453	10.3401	269	15	5
atsz–32a	Atlantic Source Zone	-59.3510	10.8123	269	15	17.94
atsz–32b	Atlantic Source Zone	-59.3734	10.3785	269	15	5
atsz–33a	Atlantic Source Zone	-58.7592	10.8785	248.6	15	17.94
atsz–33b	Atlantic Source Zone	-58.5984	10.4745	248.6	15	5
atsz–34a	Atlantic Source Zone	-58.5699	11.0330	217.2	15	17.94
atsz–34b	Atlantic Source Zone	-58.2179	10.7710	217.2	15	5
atsz–35a	Atlantic Source Zone	-58.3549	11.5300	193.7	15	17.94
atsz–35b	Atlantic Source Zone	-57.9248	11.4274	193.7	15	5
atsz–36a	Atlantic Source Zone	-58.3432	12.1858	177.7	15	17.94
atsz–36b	Atlantic Source Zone	-57.8997	12.2036	177.7	15	5
atsz–37a	Atlantic Source Zone	-58.4490	12.9725	170.7	15	17.94
atsz–37b	Atlantic Source Zone	-58.0095	13.0424	170.7	15	5
atsz–38a	Atlantic Source Zone	-58.6079	13.8503	170.2	15	17.94
atsz–38b	Atlantic Source Zone	-58.1674	13.9240	170.2	15	5
atsz–39a	Atlantic Source Zone	-58.6667	14.3915	146.8	15	17.94
atsz–39b	Atlantic Source Zone	-58.2913	14.6287	146.8	15	5
atsz–39y	Atlantic Source Zone	-59.4168	13.9171	146.8	15	43.82
atsz–39z	Atlantic Source Zone	-59.0415	14.1543	146.8	15	30.88
atsz–40a	Atlantic Source Zone	-59.1899	15.2143	156.2	15	17.94
atsz–40b	Atlantic Source Zone	-58.7781	15.3892	156.2	15	5
atsz–40y	Atlantic Source Zone	-60.0131	14.8646	156.2	15	43.82
atsz–40z	Atlantic Source Zone	-59.6012	15.0395	156.2	15	30.88
atsz–41a	Atlantic Source Zone	-59.4723	15.7987	146.3	15	17.94
atsz–41b	Atlantic Source Zone	-59.0966	16.0392	146.3	15	5
atsz–41y	Atlantic Source Zone	-60.2229	15.3177	146.3	15	43.82
atsz–41z	Atlantic Source Zone	-59.8473	15.5582	146.3	15	30.88
atsz–42a	Atlantic Source Zone	-59.9029	16.4535	137	15	17.94
atsz–42b	Atlantic Source Zone	-59.5716	16.7494	137	15	5
atsz–42y	Atlantic Source Zone	-60.5645	15.8616	137	15	43.82
atsz–42z	Atlantic Source Zone	-60.2334	16.1575	137	15	30.88
atsz–43a	Atlantic Source Zone	-60.5996	17.0903	138.7	15	17.94
atsz–43b	Atlantic Source Zone	-60.2580	17.3766	138.7	15	5
atsz–43y	Atlantic Source Zone	-61.2818	16.5177	138.7	15	43.82
atsz–43z	Atlantic Source Zone	-60.9404	16.8040	138.7	15	30.88
atsz–44a	Atlantic Source Zone	-61.1559	17.8560	141.1	15	17.94
atsz–44b	Atlantic Source Zone	-60.8008	18.1286	141.1	15	5
atsz–44y	Atlantic Source Zone	-61.8651	17.3108	141.1	15	43.82
atsz–44z	Atlantic Source Zone	-61.5102	17.5834	141.1	15	30.88
atsz–45a	Atlantic Source Zone	-61.5491	18.0566	112.8	15	17.94
atsz–45b	Atlantic Source Zone	-61.3716	18.4564	112.8	15	5
atsz–45y	Atlantic Source Zone	-61.9037	17.2569	112.8	15	43.82
atsz–45z	Atlantic Source Zone	-61.7260	17.6567	112.8	15	30.88
atsz–46a	Atlantic Source Zone	-62.4217	18.4149	117.9	15	17.94
atsz–46b	Atlantic Source Zone	-62.2075	18.7985	117.9	15	5
atsz–46y	Atlantic Source Zone	-62.8493	17.6477	117.9	15	43.82
atsz–46z	Atlantic Source Zone	-62.6352	18.0313	117.9	15	30.88
atsz–47a	Atlantic Source Zone	-63.1649	18.7844	110.5	20	22.1
atsz–47b	Atlantic Source Zone	-63.0087	19.1798	110.5	20	5
atsz–47y	Atlantic Source Zone	-63.4770	17.9936	110.5	20	56.3
atsz–47z	Atlantic Source Zone	-63.3205	18.3890	110.5	20	39.2
atsz–48a	Atlantic Source Zone	-63.8800	18.8870	95.37	20	22.1
atsz–48b	Atlantic Source Zone	-63.8382	19.3072	95.37	20	5
atsz–48y	Atlantic Source Zone	-63.9643	18.0465	95.37	20	56.3
atsz–48z	Atlantic Source Zone	-63.9216	18.4667	95.37	20	39.2
atsz–49a	Atlantic Source Zone	-64.8153	18.9650	94.34	20	22.1
atsz–49b	Atlantic Source Zone	-64.7814	19.3859	94.34	20	5
atsz–49y	Atlantic Source Zone	-64.8840	18.1233	94.34	20	56.3
atsz–49z	Atlantic Source Zone	-64.8492	18.5442	94.34	20	39.2
atsz–50a	Atlantic Source Zone	-65.6921	18.9848	89.59	20	22.1
atsz–50b	Atlantic Source Zone	-65.6953	19.4069	89.59	20	5
atsz–50y	Atlantic Source Zone	-65.6874	18.1407	89.59	20	56.3

45

Segment	Description	Longitude(^{o}E)	Latitude(^{o}N)	Strike(^{o})	Dip(^{o})	Depth (km)
atsz–50z	Atlantic Source Zone	-65.6887	18.5628	89.59	20	39.2
atsz–51a	Atlantic Source Zone	-66.5742	18.9484	84.98	20	22.1
atsz–51b	Atlantic Source Zone	-66.6133	19.3688	84.98	20	5
atsz–51y	Atlantic Source Zone	-66.4977	18.1076	84.98	20	56.3
atsz–51z	Atlantic Source Zone	-66.5353	18.5280	84.98	20	39.2
atsz–52a	Atlantic Source Zone	-67.5412	18.8738	85.87	20	22.1
atsz–52b	Atlantic Source Zone	-67.5734	19.2948	85.87	20	5
atsz–52y	Atlantic Source Zone	-67.4781	18.0319	85.87	20	56.3
atsz–52z	Atlantic Source Zone	-67.5090	18.4529	85.87	20	39.2
atsz–53a	Atlantic Source Zone	-68.4547	18.7853	83.64	20	22.1
atsz–53b	Atlantic Source Zone	-68.5042	19.2048	83.64	20	5
atsz–53y	Atlantic Source Zone	-68.3575	17.9463	83.64	20	56.3
atsz–53z	Atlantic Source Zone	-68.4055	18.3658	83.64	20	39.2
atsz–54a	Atlantic Source Zone	-69.6740	18.8841	101.5	20	22.1
atsz–54b	Atlantic Source Zone	-69.5846	19.2976	101.5	20	5
atsz–55a	Atlantic Source Zone	-70.7045	19.1376	108.2	20	22.1
atsz–55b	Atlantic Source Zone	-70.5647	19.5386	108.2	20	5
atsz–56a	Atlantic Source Zone	-71.5368	19.3853	102.6	20	22.1
atsz–56b	Atlantic Source Zone	-71.4386	19.7971	102.6	20	5
atsz–57a	Atlantic Source Zone	-72.3535	19.4838	94.2	20	22.1
atsz–57b	Atlantic Source Zone	-72.3206	19.9047	94.2	20	5
atsz–58a	Atlantic Source Zone	-73.1580	19.4498	84.34	20	22.1
atsz–58b	Atlantic Source Zone	-73.2022	19.8698	84.34	20	5
atsz–59a	Atlantic Source Zone	-74.3567	20.9620	259.7	20	22.1
atsz–59b	Atlantic Source Zone	-74.2764	20.5467	259.7	20	5
atsz–60a	Atlantic Source Zone	-75.2386	20.8622	264.2	15	17.94
atsz–60b	Atlantic Source Zone	-75.1917	20.4306	264.2	15	5
atsz–61a	Atlantic Source Zone	-76.2383	20.7425	260.7	15	17.94
atsz–61b	Atlantic Source Zone	-76.1635	20.3144	260.7	15	5
atsz–62a	Atlantic Source Zone	-77.2021	20.5910	259.9	15	17.94
atsz–62b	Atlantic Source Zone	-77.1214	20.1638	259.9	15	5
atsz–63a	Atlantic Source Zone	-78.1540	20.4189	259	15	17.94
atsz–63b	Atlantic Source Zone	-78.0661	19.9930	259	15	5
atsz–64a	Atlantic Source Zone	-79.0959	20.2498	259.2	15	17.94
atsz–64b	Atlantic Source Zone	-79.0098	19.8236	259.2	15	5
atsz–65a	Atlantic Source Zone	-80.0393	20.0773	258.9	15	17.94
atsz–65b	Atlantic Source Zone	-79.9502	19.6516	258.9	15	5
atsz–66a	Atlantic Source Zone	-80.9675	19.8993	258.6	15	17.94
atsz–66b	Atlantic Source Zone	-80.8766	19.4740	258.6	15	5
atsz–67a	Atlantic Source Zone	-81.9065	19.7214	258.5	15	17.94
atsz–67b	Atlantic Source Zone	-81.8149	19.2962	258.5	15	5
atsz–68a	Atlantic Source Zone	-87.8003	15.2509	62.69	15	17.94
atsz–68b	Atlantic Source Zone	-88.0070	15.6364	62.69	15	5
atsz–69a	Atlantic Source Zone	-87.0824	15.5331	72.73	15	17.94
atsz–69b	Atlantic Source Zone	-87.2163	15.9474	72.73	15	5
atsz–70a	Atlantic Source Zone	-86.1622	15.8274	70.64	15	17.94
atsz–70b	Atlantic Source Zone	-86.3120	16.2367	70.64	15	5
atsz–71a	Atlantic Source Zone	-85.3117	16.1052	73.7	15	17.94
atsz–71b	Atlantic Source Zone	-85.4387	16.5216	73.7	15	5
atsz–72a	Atlantic Source Zone	-84.3470	16.3820	69.66	15	17.94
atsz–72b	Atlantic Source Zone	-84.5045	16.7888	69.66	15	5
atsz–73a	Atlantic Source Zone	-83.5657	16.6196	77.36	15	17.94
atsz–73b	Atlantic Source Zone	-83.6650	17.0429	77.36	15	5
atsz–74a	Atlantic Source Zone	-82.7104	16.7695	82.35	15	17.94
atsz–74b	Atlantic Source Zone	-82.7709	17.1995	82.35	15	5
atsz–75a	Atlantic Source Zone	-81.7297	16.9003	79.86	15	17.94
atsz–75b	Atlantic Source Zone	-81.8097	17.3274	79.86	15	5
atsz–76a	Atlantic Source Zone	-80.9196	16.9495	82.95	15	17.94
atsz–76b	Atlantic Source Zone	-80.9754	17.3801	82.95	15	5
atsz–77a	Atlantic Source Zone	-79.8086	17.2357	67.95	15	17.94
atsz–77b	Atlantic Source Zone	-79.9795	17.6378	67.95	15	5
atsz–78a	Atlantic Source Zone	-79.0245	17.5415	73.61	15	17.94

| Segment	Description	Longitude(°E)	Latitude(°N)	Strike(°)	Dip(°)	Depth (km)
atsz–78b	Atlantic Source Zone	-79.1532	17.9577	73.61	15	5
atsz–79a	Atlantic Source Zone	-78.4122	17.5689	94.07	15	17.94
atsz–79b	Atlantic Source Zone	-78.3798	18.0017	94.07	15	5
atsz–80a	Atlantic Source Zone	-77.6403	17.4391	103.3	15	17.94
atsz–80b	Atlantic Source Zone	-77.5352	17.8613	103.3	15	5
atsz–81a	Atlantic Source Zone	-76.6376	17.2984	98.21	15	17.94
atsz–81b	Atlantic Source Zone	-76.5726	17.7278	98.21	15	5
atsz–82a	Atlantic Source Zone	-75.7299	19.0217	260.1	15	17.94
atsz–82b	Atlantic Source Zone	-75.6516	18.5942	260.1	15	5
atsz–83a	Atlantic Source Zone	-74.8351	19.2911	260.8	15	17.94
atsz–83b	Atlantic Source Zone	-74.7621	18.8628	260.8	15	5
atsz–84a	Atlantic Source Zone	-73.6639	19.2991	274.8	15	17.94
atsz–84b	Atlantic Source Zone	-73.7026	18.8668	274.8	15	5
atsz–85a	Atlantic Source Zone	-72.8198	19.2019	270.6	15	17.94
atsz–85b	Atlantic Source Zone	-72.8246	18.7681	270.6	15	5
atsz–86a	Atlantic Source Zone	-71.9143	19.1477	269.1	15	17.94
atsz–86b	Atlantic Source Zone	-71.9068	18.7139	269.1	15	5
atsz–87a	Atlantic Source Zone	-70.4738	18.8821	304.5	15	17.94
atsz–87b	Atlantic Source Zone	-70.7329	18.5245	304.5	15	5
atsz–88a	Atlantic Source Zone	-69.7710	18.3902	308.9	15	17.94
atsz–88b	Atlantic Source Zone	-70.0547	18.0504	308.4	15	5
atsz–89a	Atlantic Source Zone	-69.2635	18.2099	283.9	15	17.94
atsz–89b	Atlantic Source Zone	-69.3728	17.7887	283.9	15	5
atsz–90a	Atlantic Source Zone	-68.5059	18.1443	272.9	15	17.94
atsz–90b	Atlantic Source Zone	-68.5284	17.7110	272.9	15	5
atsz–91a	Atlantic Source Zone	-67.6428	18.1438	267.8	15	17.94
atsz–91b	Atlantic Source Zone	-67.6256	17.7103	267.8	15	5
atsz–92a	Atlantic Source Zone	-66.8261	18.2536	262	15	17.94
atsz–92b	Atlantic Source Zone	-66.7627	17.8240	262	15	5
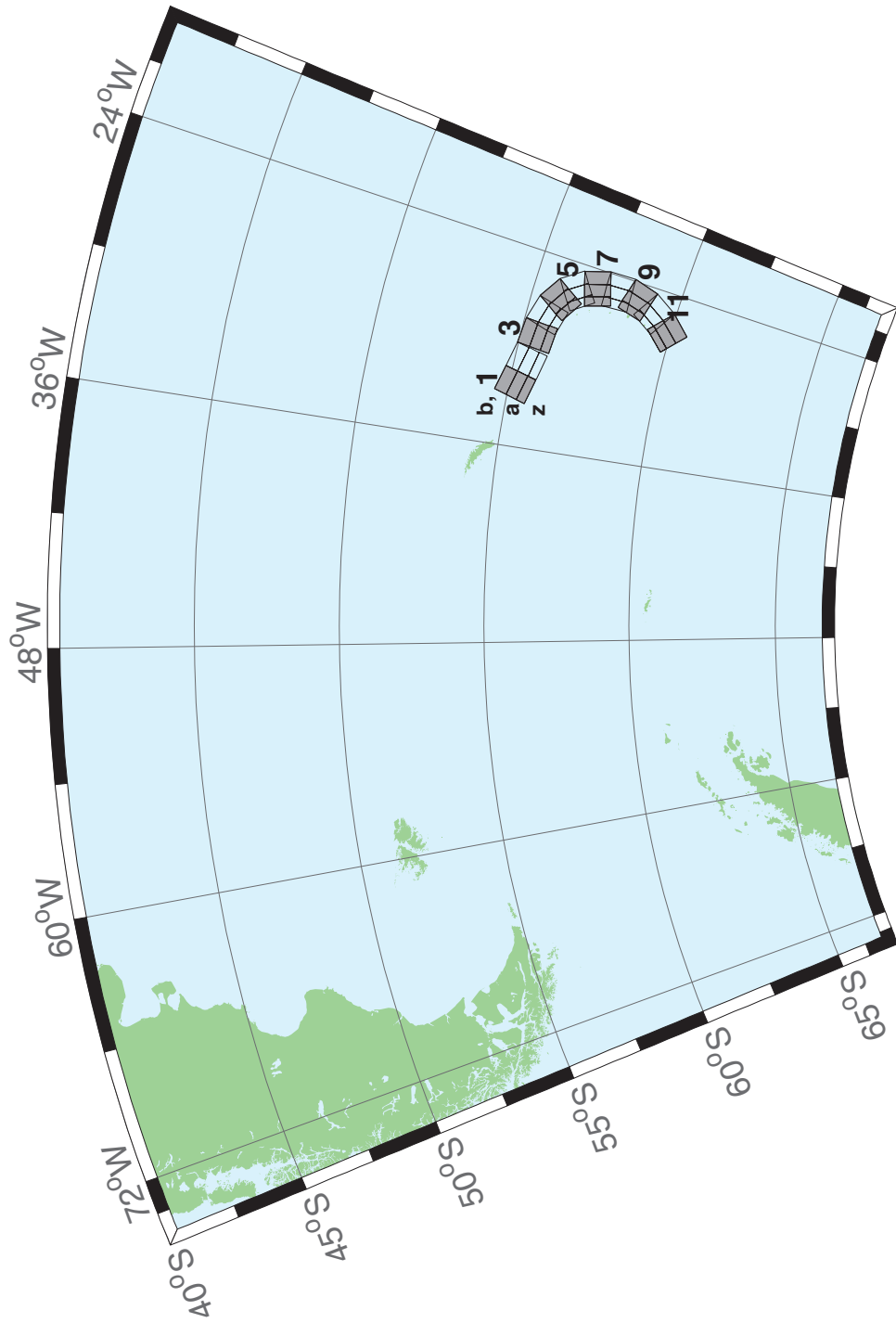
Figure B.2: South Sandwich Islands Subduction Zone.

Table B.2: Earthquake parameters for South Sandwich Islands Subduction Zone unit sources.

Segment	Description	Longitude(°E)	Latitude(°N)	Strike(°)	Dip(°)	Depth (km)
sssz–1a	South Sandwich Islands Subduction Zone	-32.3713	-55.4655	104.7	28.53	17.51
sssz–1b	South Sandwich Islands Subduction Zone	-32.1953	-55.0832	104.7	9.957	8.866
sssz–1z	South Sandwich Islands Subduction Zone	-32.5091	-55.7624	104.7	46.99	41.39
sssz–2a	South Sandwich Islands Subduction Zone	-30.8028	-55.6842	102.4	28.53	17.51
sssz–2b	South Sandwich Islands Subduction Zone	-30.6524	-55.2982	102.4	9.957	8.866
sssz–2z	South Sandwich Islands Subduction Zone	-30.9206	-55.9839	102.4	46.99	41.39
sssz–3a	South Sandwich Islands Subduction Zone	-29.0824	-55.8403	95.53	28.53	17.51
sssz–3b	South Sandwich Islands Subduction Zone	-29.0149	-55.4468	95.53	9.957	8.866
sssz–3z	South Sandwich Islands Subduction Zone	-29.1353	-56.1458	95.53	46.99	41.39
sssz–4a	South Sandwich Islands Subduction Zone	-27.8128	-55.9796	106.1	28.53	17.51
sssz–4b	South Sandwich Islands Subduction Zone	-27.6174	-55.5999	106.1	9.957	8.866
sssz–4z	South Sandwich Islands Subduction Zone	-27.9659	-56.2744	106.1	46.99	41.39
sssz–5a	South Sandwich Islands Subduction Zone	-26.7928	-56.2481	123.1	28.53	17.51
sssz–5b	South Sandwich Islands Subduction Zone	-26.4059	-55.9170	123.1	9.957	8.866
sssz–5z	South Sandwich Islands Subduction Zone	-27.0955	-56.5052	123.1	46.99	41.39
sssz–6a	South Sandwich Islands Subduction Zone	-26.1317	-56.6466	145.6	23.28	16.11
sssz–6b	South Sandwich Islands Subduction Zone	-25.5131	-56.4133	145.6	9.09	8.228
sssz–6z	South Sandwich Islands Subduction Zone	-26.5920	-56.8194	145.6	47.15	35.87
sssz–7a	South Sandwich Islands Subduction Zone	-25.6787	-57.2162	162.9	21.21	14.23
sssz–7b	South Sandwich Islands Subduction Zone	-24.9394	-57.0932	162.9	7.596	7.626
sssz–7z	South Sandwich Islands Subduction Zone	-26.2493	-57.3109	162.9	44.16	32.32
sssz–8a	South Sandwich Islands Subduction Zone	-25.5161	-57.8712	178.2	20.33	15.91
sssz–8b	South Sandwich Islands Subduction Zone	-24.7233	-57.8580	178.2	8.449	8.562
sssz–8z	South Sandwich Islands Subduction Zone	-26.1280	-57.8813	178.2	43.65	33.28
sssz–9a	South Sandwich Islands Subduction Zone	-25.6657	-58.5053	195.4	25.76	15.71
sssz–9b	South Sandwich Islands Subduction Zone	-24.9168	-58.6127	195.4	8.254	8.537
sssz–9z	South Sandwich Islands Subduction Zone	-26.1799	-58.4313	195.4	51.69	37.44
sssz–10a	South Sandwich Islands Subduction Zone	-26.1563	-59.1048	212.5	32.82	15.65
sssz–10b	South Sandwich Islands Subduction Zone	-25.5335	-59.3080	212.5	10.45	6.581
sssz–10z	South Sandwich Islands Subduction Zone	-26.5817	-58.9653	212.5	54.77	42.75
sssz–11a	South Sandwich Islands Subduction Zone	-27.0794	-59.6799	224.2	33.67	15.75
sssz–11b	South Sandwich Islands Subduction Zone	-26.5460	-59.9412	224.2	11.32	5.927
sssz–11z	South Sandwich Islands Subduction Zone	-27.4245	-59.5098	224.2	57.19	43.46

Appendix C

SIFT Testing

Authors: Nazila Merati, Yong Wei, Jean Newman

C.1   Purpose

Forecast models are tested with synthetic tsunami events covering a range of tsunami source locations. Testing is also done with selected historical tsunami events when available.

The purpose of forecast model testing is three-fold. The first objective is to assure that the results obtained with NOAA tsunami forecast system, which has been released to the Tsunami Warning Centers for operational use, are identical to those obtained by the researcher during the development of the forecast model. The second objective is to test the forecast model for consistency, accuracy, time efficiency, and quality of results over a range of possible tsunami locations and magnitudes. The third objective is to identify bugs and issues in need of resolution by the researcher who developed the forecast model or by the forecast software development team before the next version release to NOAA's two Tsunami Warning Centers.

Local hardware and software applications, and tools familiar to the researcher(s), are used to run the Method of Splitting Tsunami (MOST) model during the forecast model development. The test results presented in this report lend confidence that the model performs as developed and produces the same results when initiated within the forecast application in an operational setting as those produced by the researcher during the forecast model development. The test results assure those who rely on the Arecibo tsunami forecast model that consistent results are produced irrespective of system.

C.2   Testing Procedure

The Arecibo forecast model was tested with NOAA's tsunami forecast system version 3 with MOST v.2. The general procedure for forecast model testing is to run a set of synthetic tsunami scenarios through the forecast system application and compare the results with those obtained by the researcher during the forecast model development and presented in the Tsunami Forecast Model Report. Specific steps taken to test the model include:

1. Identify testing scenarios, including the standard set of synthetic events and customized synthetic scenarios that may have been used by the researcher(s) in developing the forecast model.

2. Create new events to represent customized synthetic scenarios used by the researcher(s) in developing the forecast model, if any.

3. Submit test model runs with the forecast system, and export the results from A, B, and C grids, along with time series.

4. Record applicable metadata, including the specific version of the forecast system used for testing.

5. Examine forecast model results from the forecast system for instabilities in both time series and plot results.

6. Compare forecast model results obtained through the forecast system with those obtained during the forecast model development.

7. Summarize results with specific mention of quality, consistency, and time efficiency.

8. Report issues identified to modeler and forecast software development team.

9. Retest the forecast models in the forecast system when reported issues have been addressed or explained.

Synthetic model runs were tested on a DELL PowerEdge R510 computer equipped with two Xeon E5670 processors at 2.93 Ghz, each with 12 MBytes of cache and 32GB memory. The processors are hex core and support hyperthreading, resulting in the computer performing as a 24 processor core machine. Additionally, the testing computer supports 10 Gigabit Ethernet for fast network connections. This computer configuration is similar or the same as the configurations of the computers installed at the Tsunami Warning Centers so the compute times should only vary slightly

C.3 Results

The Arecibo forecast model was tested with three synthetic scenarios. Test results from the forecast system and comparisons with the results obtained during the forecast model development are shown numerically in Table C.1 and graphically in Figures C.1 to C.3. The results show that the forecast model is stable and robust, with consistent and high quality results across geographically distributed tsunami sources and mega-event tsunami magnitudes. The model run time (wall clock time) was under 19 min for 8 hr of simulation time, and around 9 min for 4 hr. This run time is at the 10 min run time limit for 4 hr of simulation, satisfying time efficiency requirements.

Three synthetic events were run on the Arecibo forecast model. The modeled scenarios were stable for all cases tested, with no instabilities or ringing. Results show that the largest modeled amplitude was 14.41 m and originated in the Puerto Rico Trench (ATSZ 48-57) source zone. Amplitudes greater than 100 cm were recorded for two of three test sources. The smallest signal of 14.4 cm was recorded for the far field South Sandwich Islands (SSSZ 1-10) source. Direct comparisons of output from the forecast tool with results from available development synthetic events demonstrated that the wave patterns are similar in shape, pattern, and amplitude (the Caribbean (ATSZ 48-57) source has 1 difference and maxima differ by 11cm). The

discrepancies are mainly caused by the use of an older version of the propagation database at the time of development of the forecast model. The propagation database results are used to provide boundary conditions for the forecast models. The present SIFT testing results in Appendix C reflect the tsunami propagation database that was updated in December of 2011. It is known that the new propagation database will lead to improvement of the model results.

(a) A Grid

(b) B Grid

(c) C Grid

(d)
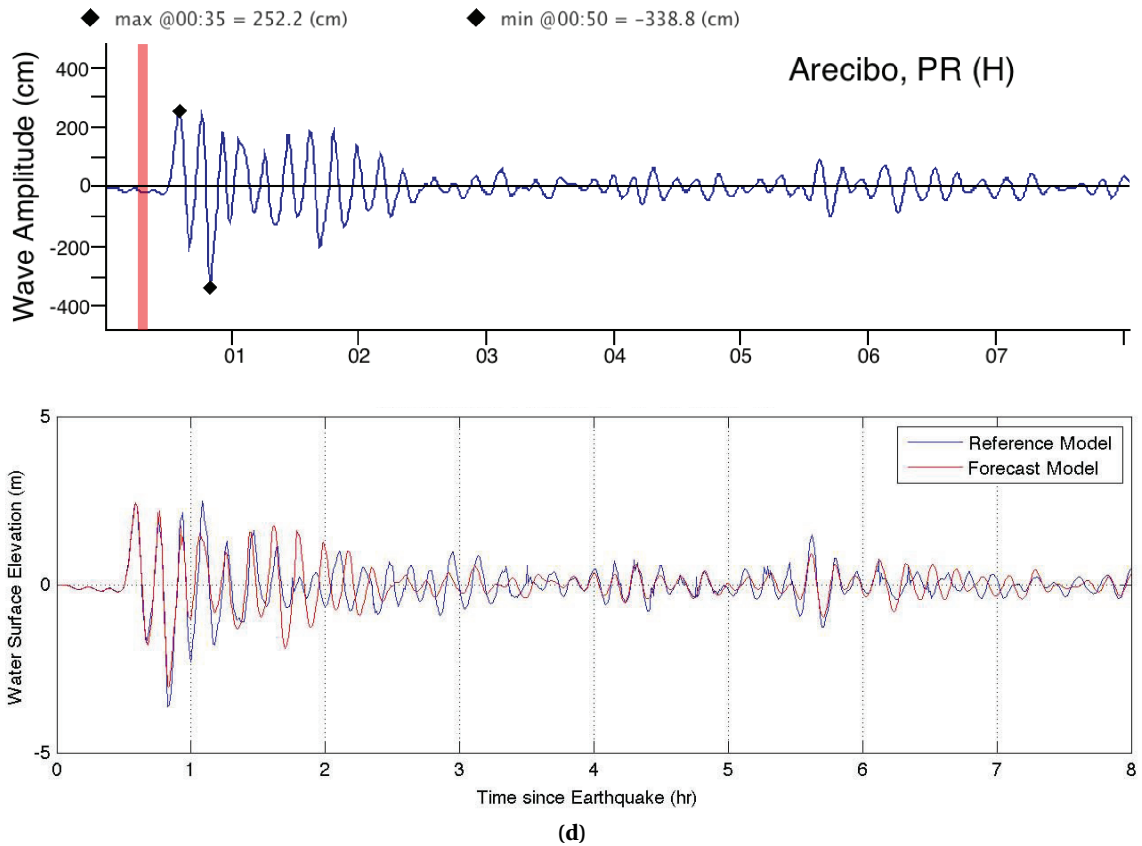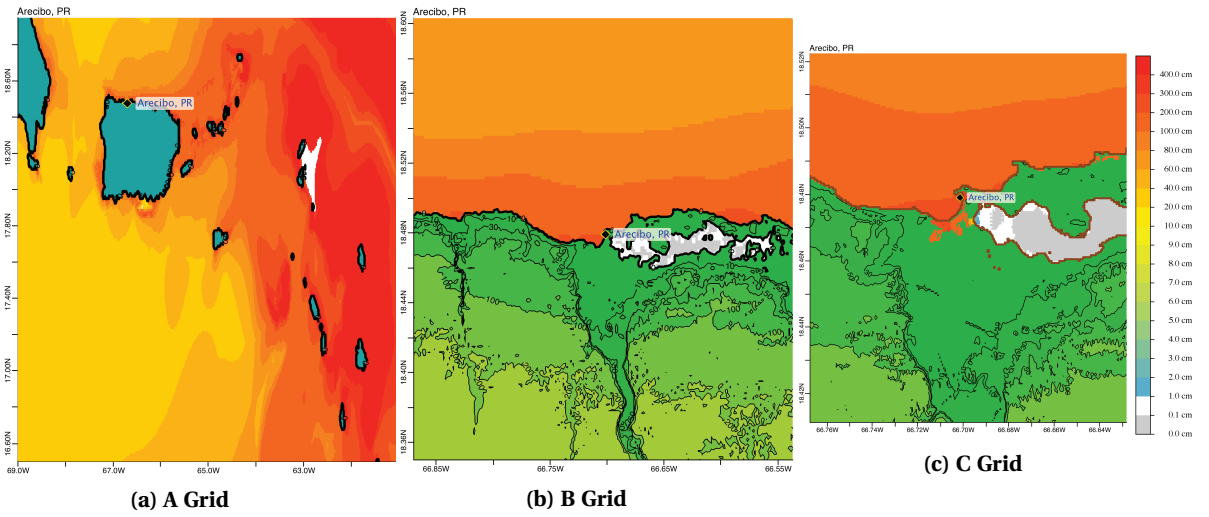
Figure C.1: Response of the Arecibo forecast model to synthetic scenario ATSZ 38-47 (alpha=25). Maximum sea surface elevation for (a) A grid, b) B grid, c) C grid. Sea surface elevation time series at the C-grid warning point (d). The bottom time series plot is the result obtained during model development and is shown for comparison with test results.

(a) A Grid

(b) B Grid

(c) C Grid

(d)
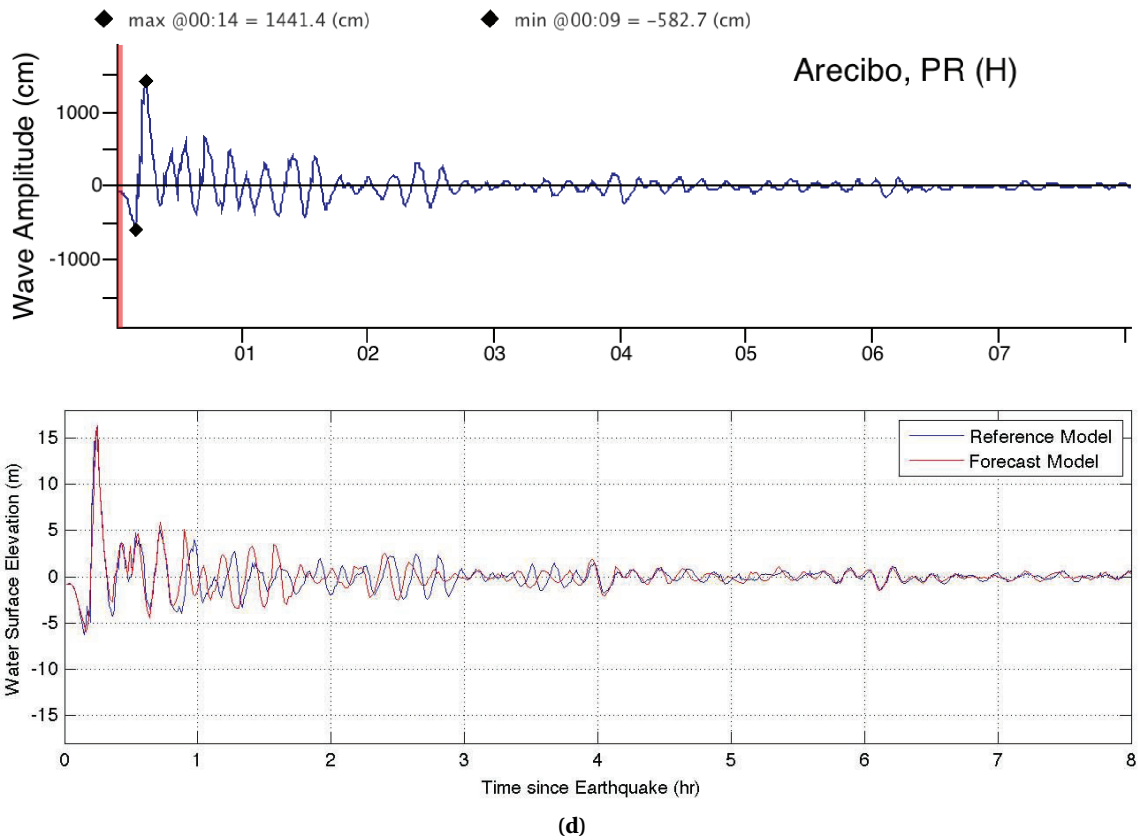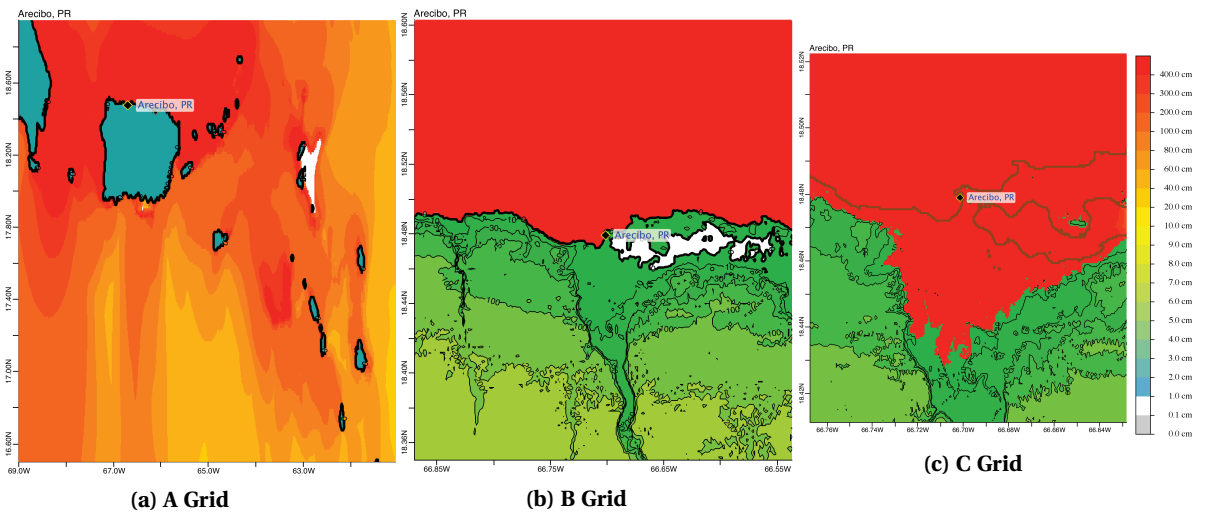
Figure C.2: Response of the Arecibo forecast model to synthetic scenario ATSZ 48-57 (alpha=25). Maximum sea surface elevation for (a) A grid, b) B grid, c) C grid. Sea surface elevation time series at the C-grid warning point (d). The bottom time series plot is the result obtained during model development and is shown for comparison with test results.

(a) A Grid
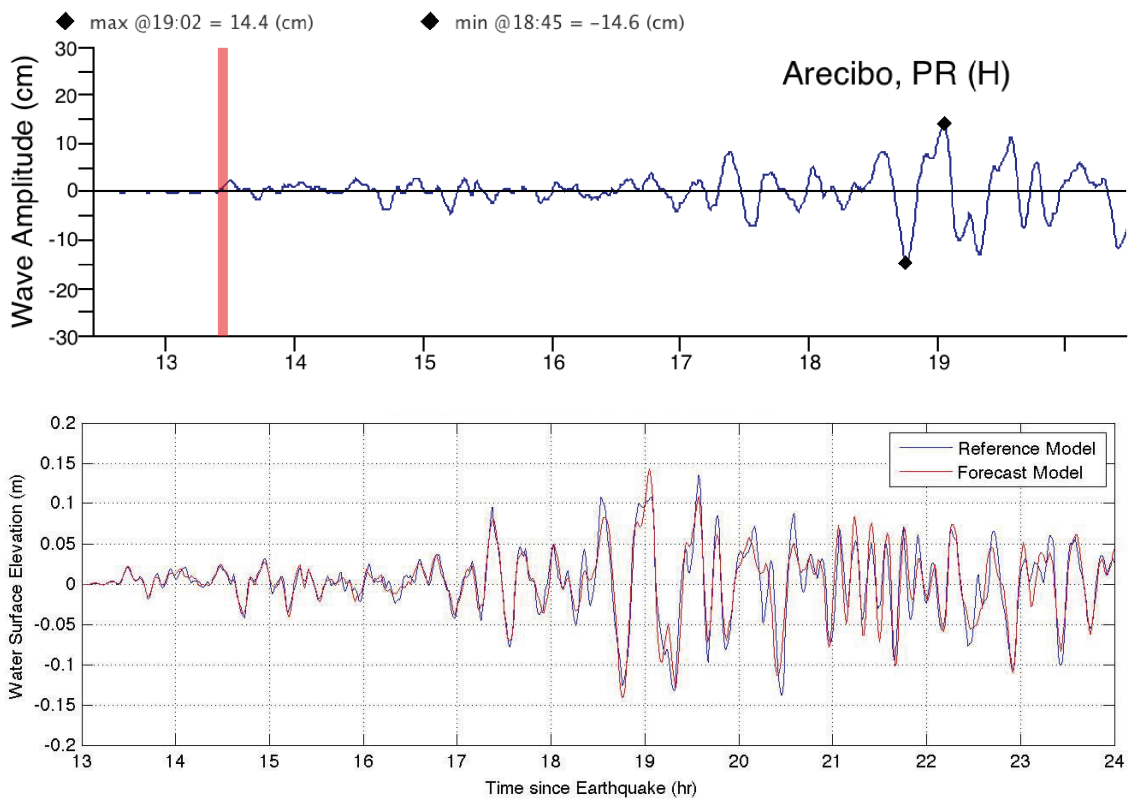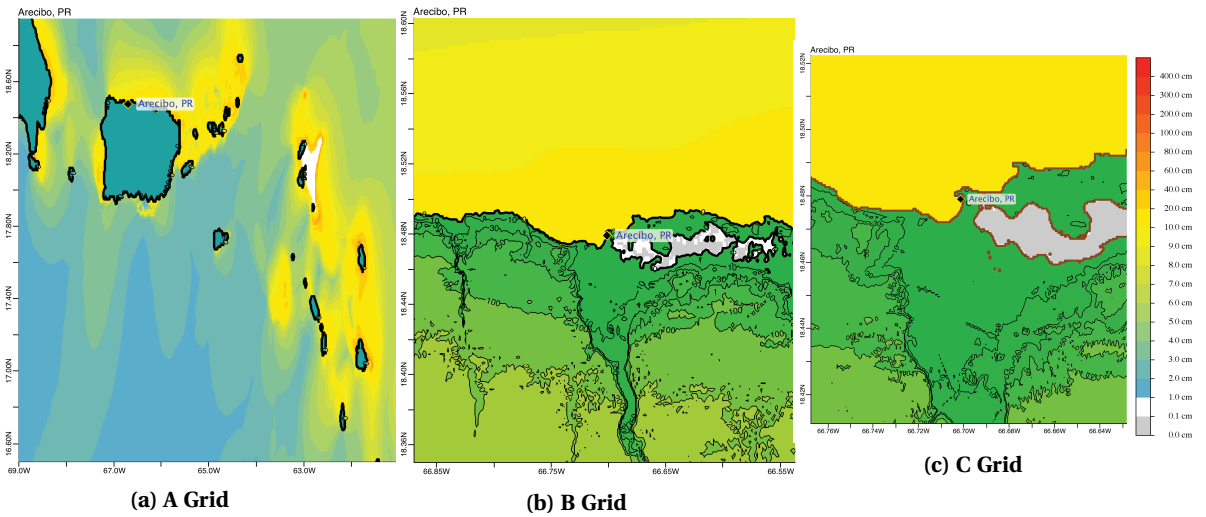
(b) B Grid

(c) C Grid

Figure C.3: Response of the Arecibo forecast model to synthetic scenario SSSZ 1-10 (alpha=25). Maximum sea surface elevation for (a) A grid, b) B grid, c) C grid. Sea surface elevation time series at the C-grid warning point (d). The bottom time series plot is the result obtained during model development and is shown for comparison with test results.

56

Table 1. Table of maximum and minimum amplitudes (cm) at the Arecibo, Puerto Rico warning point for synthetic and historical events tested using SIFT 3.2 and obtained during development.

Scenario Name	Source Zone	Tsunami Source	α [m]	SIFT Max (cm)	Development Max (cm)	SIFT Min (cm)	Development Min (cm)
Mega-tsunami Scenarios							
ATSZ 38-47	Caribbean	A38-A47, B38-B47	25	252.2	252	-338.8	-338
ATSZ 48-57	Caribbean	A48-A57, B48-B57	25	1441.4	1430	-582.7	-583
SSSZ 1-10	South Sandwich Islands	A1-A10, B1-B10	25	14.4	14	-14.6	-14

Table C.1: Table of maximum and minimum amplitudes (cm) at the Arecibo warning point for synthetic and historical events tested using SIFT 3.2 and obtained during development.

57

Appendix D

Propagation Patterns
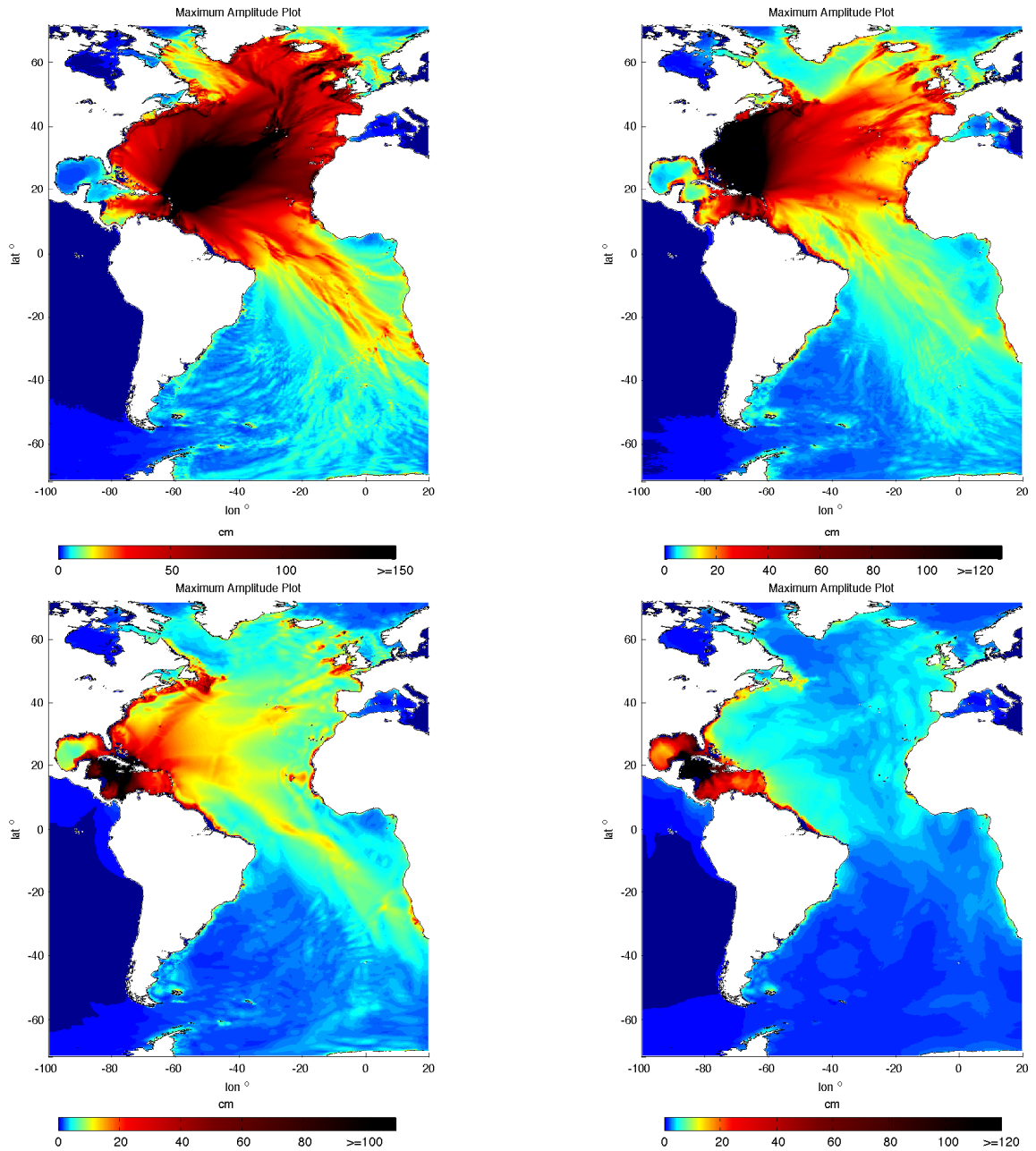
Figure D.1: Energy propagation patterns throughout the Pacific Ocean of the 8 synthetic tsunami scenarios used during the Arecibo forecast model development. Upper left panel is Scenario 1, upper right panel is Scenario 2, lower left is Scenario 3 and lower right is Scenario 4 of Table 3. Synthetic scenario 2 represents the worst case for Arecibo, situated on the northern coast of Puerto Rico.
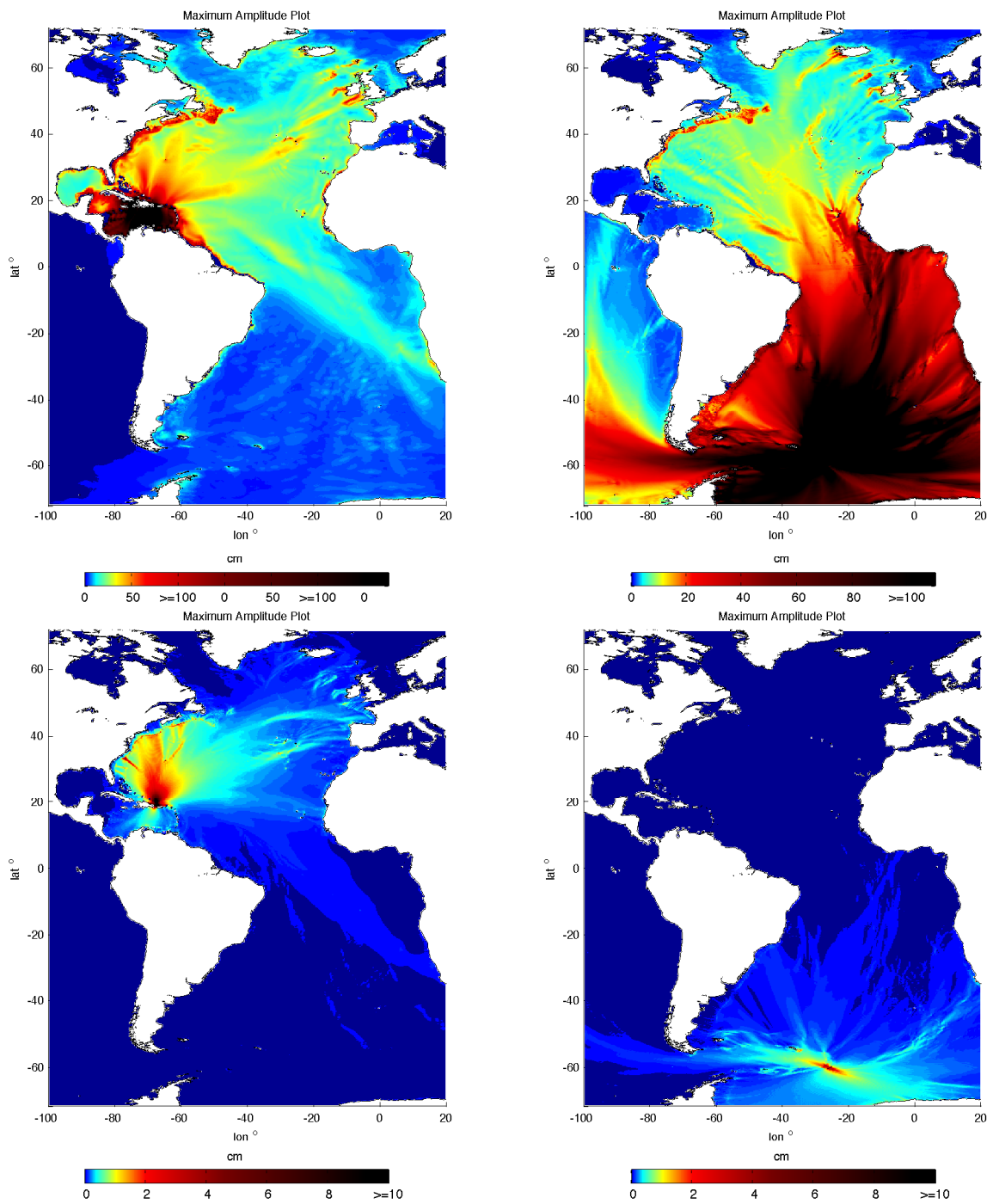
Figure D.2: Energy propagation patterns throughout the Pacific Ocean of the 8 synthetic tsunami scenarios used during the Arecibo forecast model development. Upper left panel is Scenario 5, upper right panel is Scenario 6, lower left is Scenario 7 and lower right is Scenario 8 of Table 3.